Analissa Santos Fonseca Duarte

Licenciada em Ciências de Engenharia Biomédica

The effect of UV radiation on DNA in the presence of *1,10-phenanthroline*

Dissertação para obtenção do Grau de Mestre em
Engenharia Biomédica

Orientador: Professora Doutora Maria de Fátima Guerreiro da Silva Campos Raposo, Professora Auxiliar, FCT-UNL

Júri:

Presidente: Doutora Carla Maria Quintão Pereira

Arguente: Doutora Andrea Antunes Pereira

Vogal: Doutora Maria de Fátima Guerreiro da Silva Campos Raposo

FACULDADE DE CIÊNCIAS E TECNOLOGIA
UNIVERSIDADE NOVA DE LISBOA

Dezembro, 2015

The effect of UV radiation on DNA in the presence of *1,10-phenanthroline*

“Ultimately what you do is secondary. But how you do it is primary.”

Eckhart Tolle

Acknowledgements

Firstly I would like to thank my advisor, Professora Doutora Maria Raposo for giving me the opportunity to work on this project. I am profoundly grateful for all the knowledge transmitted and the orientation given throughout the elaboration of this work. Her teachings, encouragement, mindset, and genuine humane qualities guided me, showing me that there is always another way to look at things.

To all the Professors and colleagues that somehow impacted my journey throughout these past years. I have learned and most of all grown because you have crossed my path.

To CEFITEC for providing all the necessary conditions that made the realization of this project possible. To REQUIMTE/DQ for making their laboratory and spectrophotometer available when needed. The obtained results were crucial for this work.

To the Aarhus University, Denmark, for proving access to the Synchrotron Radiation facility ASTRID, where the VUV absorption spectra were recorded.

Special thanks to all my colleagues with whom I shared the laboratory, especially to Ivan Assunção, and Crisolita Pires, who were always available to help and to give an incentive word.

To all my family and friends who always supported me throughout this process. Even though I cannot name each one of you, you are all very uniquely special and play a very important role in my life.

To my little sister, Melissa Fonseca, that even far away, remains very present in my life, always willing to listen to me and have a good laugh together. I love you!

To my PARENTS Manuel Fonseca and Filomena Santos, who have always been present in my life, and done everything on their power so that I can have a good education. THIS WORK IS DEDICATED TO YOU. Words cannot explain the love and gratitude that I have for you.

To my son Swami Duarte, who has been a part of this journey since his very first day of life. You thought me the value of time, the need to be organized, disciplined and to prioritize in order to achieve something. You have been a great master.

Lastly, I would like to thank my husband Giordano Duarte, who has always supported me. It was very important and really made a difference having your support, incentive, love, understanding, and companionship. I am grateful to have you as my life partner. Thank you!

Abstract

When designing drugs to treat diseases like cancer, which is characterized by an abnormal cellular growth, targeting the DNA seems logical in order to regulate cell functions. One possible way is to find molecules that are able to intercalate with DNA, and that in the presence of UV radiation will induce specific DNA lesions. These lesions could affect processes such as DNA transcription and replication, contributing to the non-proliferation of cancer cells. On this dissertation the influence of the intercalator *1,10-phenanthroline* (Phen) on DNA degradation was analyzed in the presence of UV radiation, 254 nm. The damages caused by UV radiation were studied by vacuum ultraviolet (VUV), ultraviolet-visible (UV-Vis), and Fourier transform infrared (FTIR) spectroscopy. The obtained results showed that the presence of water is essential in order to observe the effect of UV radiation. Both DNA and Phen were degraded when exposed to UV radiation. Through FTIR characterization it was possible to conclude that despite the fact that Phen had a degrading effect on some DNA components, it generally had a protective effect on most of the DNA components.

Keywords: DNA, 1,10-phenanthroline, UV radiation, FTIR, UV-Vis, and VUV.

Resumo

Ao desenvolver medicamentos para tratar doenças como o cancro, que é caracterizado por um crescimento celular anormal, parece lógico ter-se como alvo o ADN para que se consiga regular as funções celulares. Uma possível alternativa é encontrar moléculas que são capazes de se intercalar com o ADN e que na presença de radiação UV vão induzir lesões específicas no mesmo. Essas lesões poderão afectar processos tais como a transcrição e replicação do ADN, contribuindo para a não proliferação de células cancerígenas. Nesta dissertação analisou-se a influência do intercalante *1,10-phenanthroline* em presença de radiação UV, 254 nm, na degradação do ADN. Os danos causados pela radiação UV foram analisados pelas técnicas de espectroscopia ultravioleta de vácuo (VUV), ultravioleta-visível (UV-Vis), e infravermelho por transformada de Fourier (FTIR). Os resultados obtidos mostraram que a presença da água é essencial para que se possa observar o efeito da radiação UV. Através da caracterização por FTIR foi possível concluir que embora o intercalante tenha um efeito degradante em alguns dos componentes do ADN, no geral apresenta uma acção mais protectora do que destruidora do ADN.

Palavras-chave: ADN, *1,10-phenanthroline*, radiação UV, FTIR, UV-Vis, e VUV.

Contents

Figure Contents

Table Contents

Abbreviations and Symbols

(6-4)PPs	Pyrimidine (6-4) Pyrimidine Photoproducts
$^1O_2$	Singlet Oxygen
A	Adenine
Abs	Absorbance
C	Cytosine
CaF_2	Calcium Fluoride
CAS	Chemical Abstracts Service
CEFITEC	Centre of Physics and Technological Research
CPDs	Cyclobutane Pyrimidine Dimers
D	Dose of Irradiation
DNA	Deoxyribonucleic Acid
DQ	Department of Chemistry
FTIR	Fourier Transform Infrared
G	Guanine
H_2O_2	Hydrogen Peroxide
H_2SO_4	Sulfuric Acid
He	Helium

I	Irradiance
IR	Infrared
M	Molar (mol/L)
MB	Methylene Blue
MΩ	Mega Ohm
PDT	Photodynamic Therapy
Phen	1,10-phenanthroline
R	Correlation coefficient
REQUIMTE	Rede de Química e Tecnologia
RNA	Ribonucleic Acid
ROS	Reactive Oxygen Species
T	Thymine
UV	Ultraviolet
UVA	Ultraviolet A
UVB	Ultraviolet B
UVC	Ultraviolet C
UV-Vis	Ultraviolet-visible
V	Volt
VUV	Vacuum Ultraviolet
W	Watt
α	Alpha angle
ε	Absorption coefficient
σ	Sigma
τ	Time constant
φ	Radiation flux

1

Introduction

According to the National Cancer Institute [1], cancer is among the most leading causes of death worldwide. In 2012, there were 14 million new cases and 8.2 million cancer-related deaths worldwide, and the number of new cancer cases is estimated to rise to 22 million within the next two decades. When facing the statistics, the urgency to find new ways of preventing and treating cancer diseases becomes very clear.

The discovery of the double helix structure of the deoxyribonucleic acid (DNA) by Watson and Crick brought new light on how the genetic information is stored and transmitted from generation to generation. The information on how this genetic information is expressed and how to stimulate and prevent gene expression is crucial to finding new anticancer drugs and treatments [2]. The DNA molecule structure can be disrupted by the insertion of planar aromatic molecules into the DNA helix. This process is called intercalation, and results in significant conformational changes of the DNA structure which may cause functional changes. These changes may prevent the replication of DNA and therefore inhibit the growth of cancer cells or ultimately lead to cell death [3].

The process of DNA intercalation was first discovered by Lerman [4] in 1961 through his studies into the binding of acridines to DNA. Since then, a considerable number of organic, inorganic octahedral and square planar compounds have been developed as anticancer and diagnostic agents [5].

Intercalators can then be used as anticancer drugs utilized in photodynamic therapy (PDT). In PDT the cells are targeted by a photosensitizer (intercalator). When exposed to a light source in the presence of oxygen, the photosensitizer is activated and reactive oxygen species (ROS) are formed, which result in cellular destruction [6].

Rocha [7] recently studied the intercalator methylene blue (MB) and found that it has a protective effect on DNA. When irradiated with ultraviolet (UV) light and in the absence of the intercalator, the adenine and thymine bases suffered damages. However, in the presence of MB there were minimal damages, which confirm the protective effect that the intercalator has on DNA. Regarding the other bases, cytosine and guanine, they were degraded both in the presence and absence of MB.

Neves [8], on the other hand, studied the mechanisms of interaction between DNA and the intercalator 2,2'-bypiridil in the presence of UV radiation. The results showed that in the presence of the intercalator, there is a more rapidly DNA degradation, and therefore 2,2'-bypiridil may be a possible candidate to induce DNA lesions.

This project aims to understand the influence of the intercalator, 1-10-phenantroline (Phen), on DNA degradation. The effect of UV radiation on the intercalator-DNA mixture will be studied by ultraviolet-visible (UV-Vis) spectroscopy of aqueous solutions of the compounds; and Fourier transform infrared (FTIR), and vacuum ultraviolet (VUV) spectroscopy of cast films irradiated for different time intervals.

This dissertation is divided into seven chapters. In chapter two there will be presented the information necessary to understand some concepts that will be mentioned throughout this thesis, such as the mechanisms of interaction between UV radiation and matter, photodynamic therapy, and intercalators and their mechanisms of interaction. The experimental procedure is presented in chapter three, where the methods to prepare the solutions and samples are described, as well as the characterization techniques. The characterization is done by VUV, UV-Vis and FTIR spectroscopy, and the results are presented in chapter four, five, and six respectively. The conclusions are presented in chapter seven.

2

The effect of radiation on DNA and Intercalators

2.1 DNA molecule and UV radiation

The discovery of the DNA structure by James Watson and Francis Crick in 1953 was responsible for significant scientific advances. The structure of DNA was crucial to unveil some fundamental information, like the mechanism whereby the hereditary information is copied for transmission from cell to cell, and how proteins are specified by the instructions in the DNA [9]

The DNA molecule is composed of two long polynucleotide strands wound into a helix. Each of these strands is composed of four types of subunits known as nucleotides. DNA nucleotides (**Figure 2.1**) are composed of a five-carbon sugar (deoxyribose), to which is attached one or more phosphate groups and a nitrogen-containing base, that may be either adenine (A), cytosine (C), guanine (G), or thymine (T). A and G are purine bases while C and T are pyrimidine bases [10].

Hydrogen bonds between the base portions of nucleotides on opposite strands are what hold the two DNA chains together. The pairing of these bases does not occur at random. Adenine always pair with thymine, and guanine with cytosine. The nucleotides that make up one strand are covalently linked together through the sugars and phosphates. It is the way that these nucleotides are linked that gives the DNA strand its polarity, indicated by referring to one end as the 3' end (the one with the phosphate) and the other as the 5' end (the one with the sugar). Considering the polarity of each strand, the complementary base-pairing is only possible because the two DNA strands are antiparallel (run in opposite directions) [9].

The surface of the double helix contains two grooves of unequal width: the major and minor groove. The major groove is narrow and deep, while the minor groove is wide and shallow[10]. The structure of DNA is shown in **Figure 2.2**.

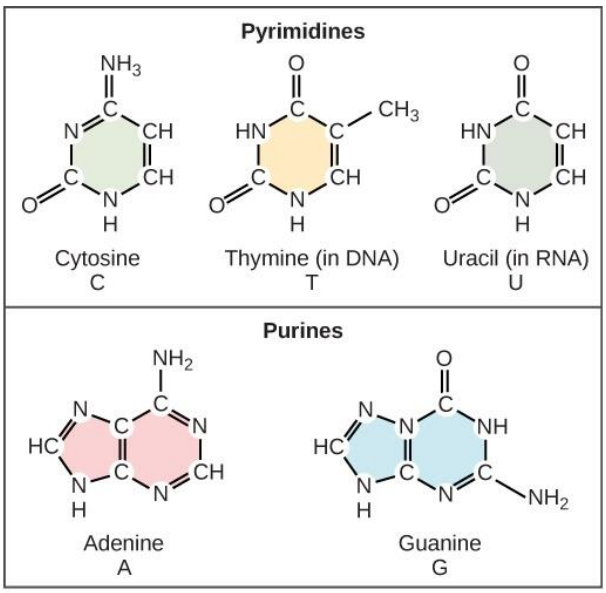

Figure 2.1: DNA nucleotides (Adapted from [11]).

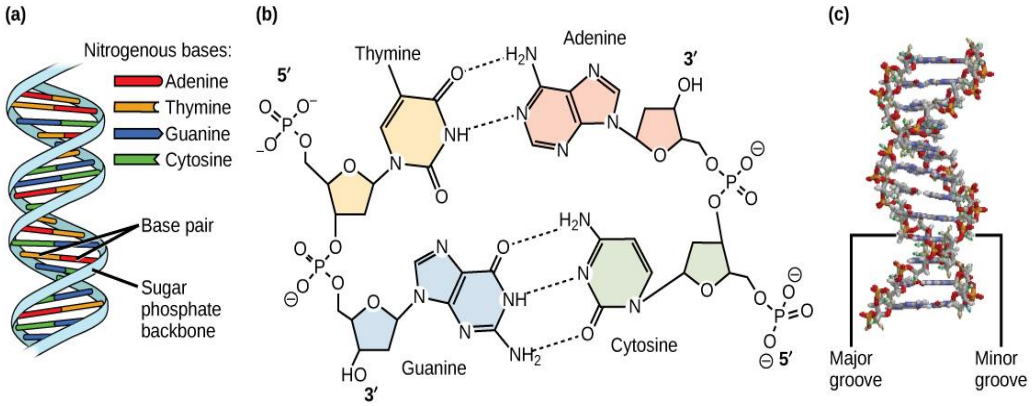

Figure 2.2: Molecular structure of DNA: a) DNA double helix, b) partial chemical structure showing the complementary strands of DNA, and c) major and minor grooves (Adapted from [11]).

DNA can be considered the molecule of life, which stores, replicates and transmits the genetic information from generation to generation. The DNA sequence is transcribed onto ribonucleic acid (RNA) biomolecules that will be used in translation- protein synthesis to encode a specific protein sequence [3].

The DNA structure can be altered when exposed to mutagens, such as ultraviolet (UV) radiation, which may lead to the formation of mutagenic DNA lesions and even cell death. The UV radiation spectrum is divided into different region (**Figure 2.3**): ultraviolet A-UVA (320-400 nm), ultraviolet B-UVB (280-320 nm), ultraviolet C-UVC (200-280), and vacuum ultraviolet- VUV (200-100 nm). Different wavelengths of UV light have different mutagenic properties [12].

The UVC (200-280 nm) can be considered the most effective in inducing DNA lesions, the reason being that DNA has its peak of light absorption at 260 nm. For this reason, and for being the most energetic radiation, exposure to UVC should cause concern. However UVC is completely absorbed by ozone and oxygen, which prevents it from reaching the Earth's surface [13].

The major DNA lesions caused by UVC and UVB are pyrimidine dimers, which are caused by direct excitation of the DNA molecule. These dimers can be of two types: the cyclobutane pyrimidine dimers (CPDs) and pyrimidine (6-4) pyrimidine photoproducts [(6-4)PPs] (**Figure 2.4**). However, CPDs account for the majority of mutations induced by UVB irradiation. DNA can also be damaged indirectly by radicals, mainly reactive oxygen species (ROS). Oxidative DNA damage is caused primarily by UVA. Studies have shown that the genotoxicity of UV radiation is due to a great extent to the formation of pyrimidine dimers, and when concerning biological effects such as DNA inactivation, oxidative damages may be less significant [12][13].

Cellular processes such as transcription and DNA replication can be affected by pyrimidine dimer lesions causing mutations or even cell death. However, DNA has its own repair mechanisms, and in the case of pyrimidine dimer lesions, they are removed by excision repair. UV "signature" mutations are mutations caused by DNA UV-induced lesions, and are in the form of CT and CCTT transitions [14].

Pyrimidine dimers often occur in adjacent thymine, even though they may occur between cytosine and guanine. This is due to the fact that thymine-adenine double bond (T=A) requires less energy to be broken than the cytosine-guanine triple bond (C≡G). Only rarely does the DNA replication and repair processes fail and allow mutation to occur in the DNA. However if sufficient pyrimidine dimers are created, the DNA is unable to replicate. DNA damage, such as thymine dimers frequently stop the DNA replication at the site of the damage, therefore the inhibitory effect of UV radiation is more relevant in cell growth than its mutagenic effect [9].

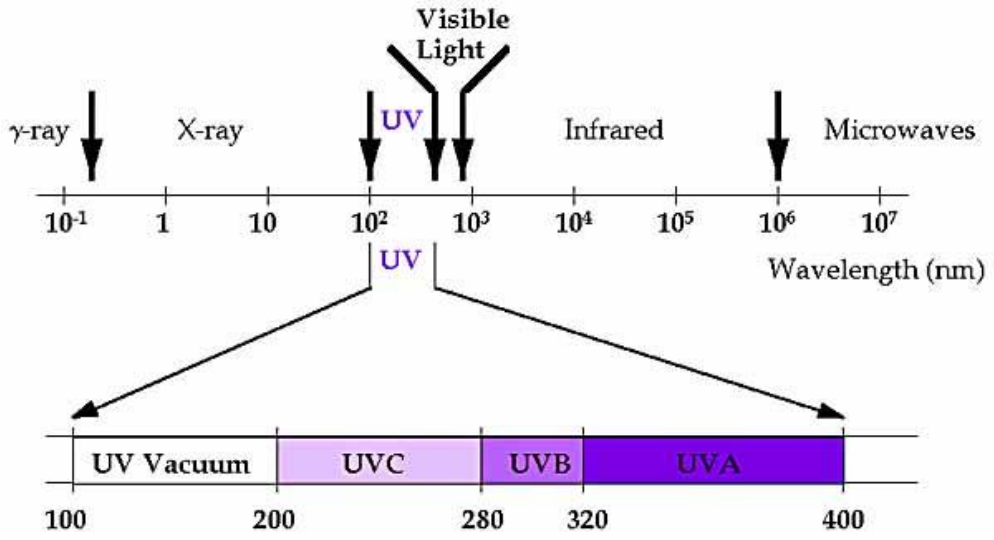

Figure 2.3: The ultraviolet portion of the electromagnetic spectrum (Adapted from [14]**).**

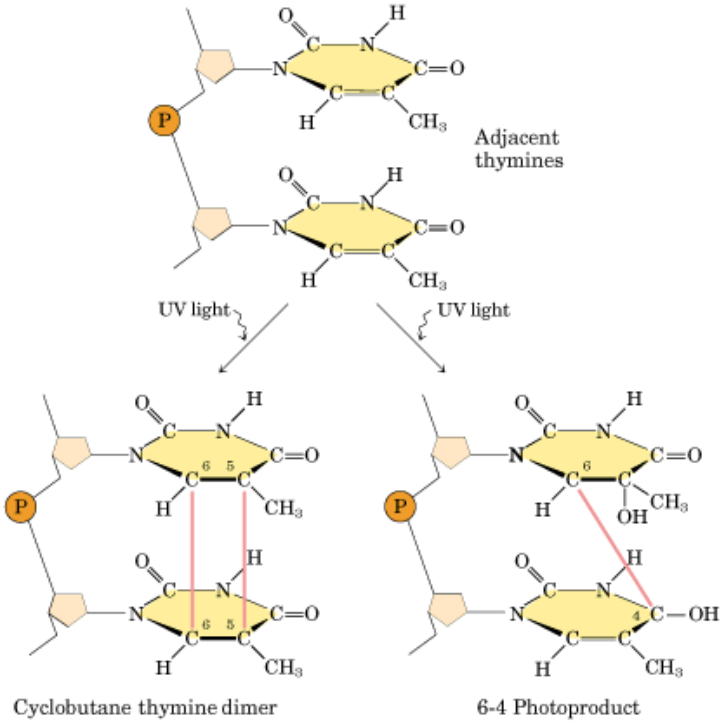

Figure 2.4: Different lesions that occur at adjacent pyrimidine residues when exposed to UV light [15]**.**

2.2 Photodynamic Therapy (PDT)

Photodynamic therapy is a therapeutic method used to treat different types of cancer and other pathologies. Depending on the location and stage of the disease, PDT may present many advantages when compared to other interventions, such as surgery and radiotherapy: it can be targeted accurately, repeated doses can be given without the total-dose limitations associated with radiotherapy, and the healing process results in little or no scarring [16].

In PDT a light source, oxygen, and photosensitizers are combined to induce damage in the selected tissue. The idea that this combination could produce cellular damage was discovered accidentally by a medical student, Oscar Raab, who observed that the presence of the photosensitizer acridine orange and light together had a toxic effect on *Paramecium caudatum cells* [6].

PDT is based on the administration of a non-toxic dye (photosensitizer) to a specific lesion, either systemically, locally, or topically, which is then exposed to a light source, in the presence of oxygen. Only cells targeted by the photosensitizer are destroyed, which makes PDT a specific and selective treatment. The presence of molecular oxygen plays a key factor in the success of PDT, because when the photosensitizer is activated by light, reactive oxygen species (ROS) are generated, which lead to a series of oxidative events that result in cellular destruction [17].

When the photosensitizer is exposed to light, it is activated from a ground state to an excited state. Cell killing can be induced in two ways, as the photosensitizer returns to its ground state (**Figure 2.6**). It can react directly with a substrate such as the cell membrane or a molecule, and produce radicals, which may further react with oxygen to produce ROS (Type I reaction). Alternatively the photosensitizer can transfer its energy directly to oxygen to form singlet oxygen (Type II reaction). In PDT, type II reactions are thought to occur more frequently [6].

Singlet oxygen ($^1O_2$) is very reactive and also has a short half-life, which means that only molecules that are close to the region of its production are affected and destroyed by PDT [17]. In order to prevent damage to surrounding healthy tissue it is important to act on PDT selectivity, which is influenced by factors like uptake of the photosensitizer into target cells/tissue; metabolism of the agent to its active form; and penetration and selectivity of the light source [6]. Certain characteristics should be considered when selecting a photosensitizer, like chemical and physical stability, short time interval between administration and maximal accumulation within tumor tissues, activation at wavelength with optimal tissue penetration, and rapid clearance from the body [18].

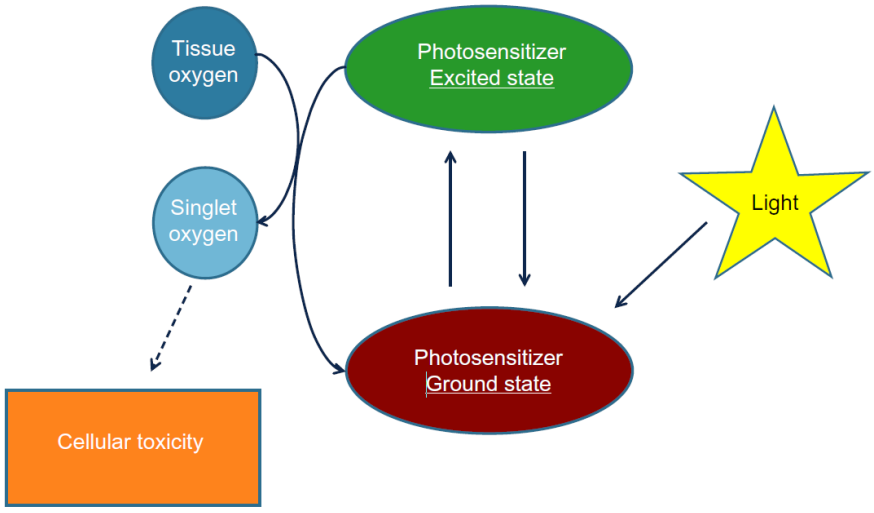

Figure 2.5: Schema of a photochemical reaction during a photodynamic therapy (Adapted from [6]).

2.3 Intercalators

Understanding the mechanisms of interaction between drug molecules and DNA, is a crucial step to develop DNA-targeted drugs that can interfere in cell functions such as transcription and replication. Anti-cancer drugs specifically may interact with DNA through control of transcription factors and polymerases, through RNA binding to DNA double helix to form nucleic acid triple helix structures or RNA hybridization to exposed DNA single strand forming DNA-RNA hybrids that may interfere with transcriptional activity, and through binding of small aromatic ligand molecules to DNA double helical structure. Drug-DNA binding may occur covalently or non-covalently. The covalent binding of a drug molecule to DNA is irreversible and leads to an inhibition of the DNA processes resulting in cell death. On the other hand non-covalent drug-DNA interaction is reversible and less cytotoxic when compared to covalent binding. Nevertheless, non-covalent interacting agents may cause significant DNA conformational changes that may result in a hindered or suppressed function of DNA [19].

Small molecules may bind non-covalently to DNA by two common binding modes; intercalation and groove-binding (**Figure 2.5**). Groove-binders are usually narrow curved shaped and fit into the DNA minor groove by van der Walls interaction and hydrogen bonding, with little distortion of the DNA structure [3].

Intercalation can be defined as the sliding-in of planar heterocyclic molecules between sequential base pairs of DNA. The interaction between the intercalator and the adjacent DNA base pairs is stabilized by the overlap of the π clouds of both [3][20].

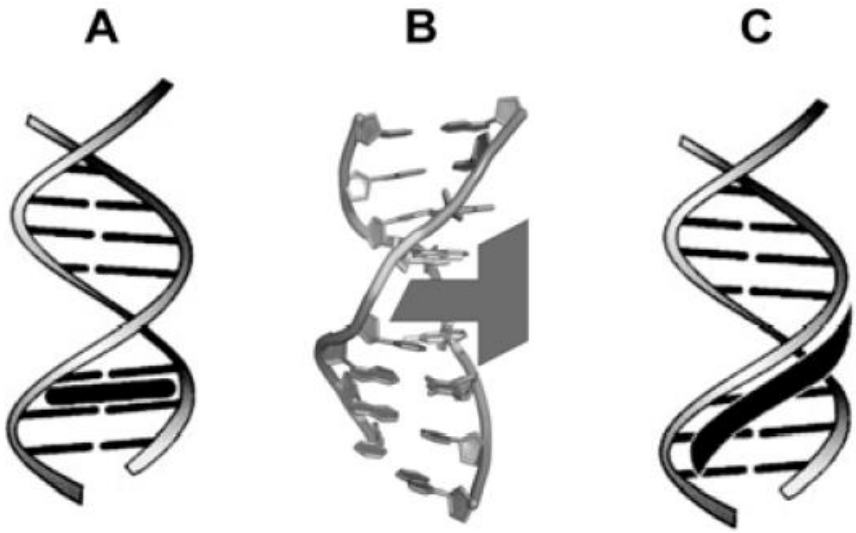

Figure 2.6: A- Generic intercalation representation; B-Schematic representation of a general intercalating agent; C-Groove binding representation (Adapted from [3]**).**

Upon insertion of the intercalator, DNA unfolds in order for the intercalator to fit between the base pairs. The unwinding of the double strand results in distortions on the DNA structure, such as, lengthening or twisting of the base pairs of the DNA strand. DNA structural changes caused by intercalators, make them potent mutagens, since these changes may lead to functional alterations like the inhibition of transcription and replication, and DNA repair processes [3][21].

Unlike many chemotherapeutic drugs, intercalators do not bind covalently to the purine and pyrimidine bases. Consequently they can be used as photosensitizers- molecules that are activated by light- targeting only tumorous cells, while preserving the normal cells from their toxic effect [22].

Since the studies of Lerman, who reported the intercalation process through the binding of acridines to DNA, other organic intercalators have been reported. Even though the number is extensive, all of the organic intercalators have chemical structures that can be divided into six different categories: anthracenes, acridines, anthraquinones, phenanthridines, phenanthrolines, and ellipticines (**Figure 2.7**) [5].

An example of an organic intercalator is daunorubicin, a potent anti-cancer drug. As well as daunorubicin, there are other organic intercalators approved by the FDA for the treatment of cancers, namely doxorubicin, mitoxantrone, and amsacrine [5].

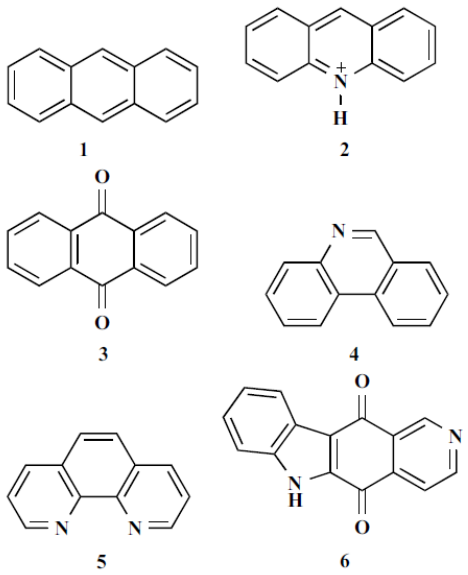

Figure 2.7: Chemical structure of organic intercalators: (1) anthracenes, (2) acridines, (3) anthraquinones, (4) phenanthridines, (5) phenanthrolines, and (6) ellipticines [5].

In PDT it is important to understand the mechanisms of interaction between the DNA molecule and the intercalator when subjected to radiation. The understanding of these interactions is crucial to optimize the destruction of the cancerous cells when exposed to UV radiation in the presence of the intercalator.

Rocha studied the effect of UV radiation on DNA, in the presence of the intercalator methylene blue (MB). The interaction of MB with the isolated DNA bases was also studied in order to comprehend how this intercalator may induce DNA lesions. MB has a protective effect on the DNA, prolonging the time necessary for its degradation when exposed to UV radiation. Regarding the bases, MB had a protective effect on adenine and thymine, but on the other hand it increased the degradation of cytosine and guanine [7].

Neves studied the DNA damage caused by UV radiation in the presence of the intercalator 2,2'-Bipyridil. The DNA degradation of the DNA is accentuated in the presence of 2,2'-Bipyridil, affecting all bases mainly guanine. FTIR characterization showed that 2,2'-Bipyridil contributes to accentuate the damage on different DNA components, although it may have a protective effect in some cases. The results suggest that 2,2'-Bipyridil might be a possible candidate for inducing DNA damage.

3

Materials and Methods

3.1 Materials

3.1.1 Deoxyribonucleic acid sodium salt from calf thymus (DNA)

The DNA purchased from Sigma-Aldrich (CAS 73049-39-5), is prepared from calf thymus tissue. It contains both single and double stranded forms of DNA, but the predominant form is the double stranded form. The molecular structure of DNA is shown in **Figure 2.2**.

DNA in the form of sodium salt has a sodium ion as a counterion which facilitates its dissolution in water, making it possible to prepare aqueous DNA solution.

3.1.2 1,10-Phenanthroline (Phen)

1,10-Phenanthroline, obtained from Alfa Aesar (CAS 66-71-7) is a heterocyclic organic compound that has the appearance of a white solid at room temperature, and a molecular weight of 180.21 g/mol. It can be used as a ligand in coordination chemistry [23]. The molecular structure of Phenanthroline- empirical formula $C_{12}H_8N_2$- is represented in **Figure 3.1**.

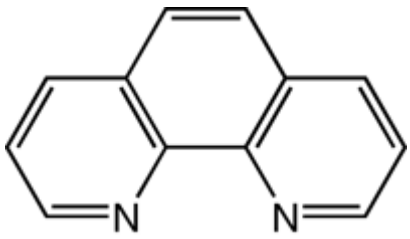

Figure 3.1: 1,10- Phenanthroline (Adapted from [24]**).**

3.2 Sample Preparation

3.2.1 Solutions

Aqueous solutions were prepared by dissolving the solute in ultra-pure water, using a Millipore system, which produces standard water of the type Mili-Q, with a resistivity of 18.2 MΩ.cm, at a temperature of 25 ºC.

An aqueous solution of 1,10- Phenanthroline (Phen)- CAS 66-71-7- was prepared by dissolving Phen in ultra-pure water to a concentration of 2×10^{-5} M. Similarly, an aqueous solution of deoxyribonucleic acid sodium salt from calf thymus (DNA)- CAS 73049-39-5- was prepared by dissolving DNA in ultra-pure water to a concentration of 0.025 mg/mL.

The prepared solutions of DNA, Phen, and [1:1](v/v) DNA+Phen were irradiated in sealed quartz cuvettes, and characterized by UV-Vis spectroscopy. Since water was the solvent used to prepare the solutions, a quartz cuvette with water was used as reference.

3.2.2 Washing and storage of the substrates

Calcium fluoride (CaF_2) substrates were used to produce cast films since calcium fluoride is transparent to infrared in the region of 4000 cm^{-1} to 600 cm^{-1}. The following steps were taken in order to ensure that the substrates were properly cleaned:

- Wash with common soap;
- Wash with a solution of methanol/acetone/chloroform to remove any trace material previously deposited onto the CaF_2 substrates;
- Immersion in a solution of H_2SO_4:H_2O_2 in a 1:1 proportion. This solution is called a piranha solution because it cleanses any residue of organic material off the substrates, and will also hydrolyze their surfaces;

  ***Warning**: Proper safety measurements should be taken when handling and preparing the piranha solution which is very corrosive and results in an exothermic reaction. The solution should be prepared in a hotte, and allowed to cool before the immersion of the substrates, to avoid possible fragmentation.*

- Wash with ultra-pure water;
- Drying with nitrogen gas.

3.2.3 Preparation of cast films

Cast films with different solutions were prepared in order to be characterized by vacuum ultraviolet (VUV) and Fourier Transform Infrared (FTIR) spectroscopy. **Table 3.1** lists the aqueous solutions that were used in the preparation of the cast films.

The solutions were deposited onto calcium fluoride substrates with the help of a pipette making sure that the dispensed amount of solution was properly distributed onto the substrate. The substrates were then left to dry in a desiccator for a period of 24h, so that the solvent could evaporate.

The cast films that were characterized by FTIR were irradiated in the presence of water, by having a recipient with water inside the UV radiation chamber increasing its moisture. The samples were characterized before and after each exposure to UV radiation.

Table 3.1: Solutions used for the preparation of cast films

Characterization	Sample	Ratio
FTIR	DNA	1.38 mg/mL
	Phen	0.18 mg/mL
	DNA+ Phen	[1:1](v/v)
VUV	DNA	0.05 mg/mL
	Phen	0.36 mg/mL
	DNA+ Phen	[4:1](v/v)

3.3 Irradiation Source

To study the effect of radiation on the prepared solutions of DNA and the intercalator 1,10- Phenanthroline, an ultraviolet system was used. The system is composed by a UVC germicidal lamp (*Philips TUV PL-S 5W/2P 1CT*). This low pressure mercury discharge lamp of cylindrical geometry has a technical wattage of 5.5 W, a voltage of 34 V, and a UVC radiation of 1.1 W. It should be referred that the UVC germicidal lamp emits UV radiation at 254 nm wavelength. With this wavelength approximately 85% of the maximum germicidal effect is obtained. The emission of radiation in this range of wavelengths induces the production of ozone, which is toxic and highly reactive, this being the reason why the lamp has a glass which filters out the 185 nm line of the mercury [25][26].

The system possesses a ventilation chamber for ozone removal, and a security system which only allows the lamp to be on if the door is closed. This ensures the security of the user who is not exposed to UVC radiation since the germicidal effect of UVC radiation can cause temporarily conjunctivitis (inflammation of the mucous membrane of the eye) and erythema (redness of the skin). Proper caution should be taken while handling the equipment, like the use of appropriate gloves and googles. The system also encompasses an adjustable sample holder allowing to vary the distance between the sample and the light source, and thus adjust the irradiance to which the sample is exposed [26].

The scheme of the system is shown in **Figure 3.2**.

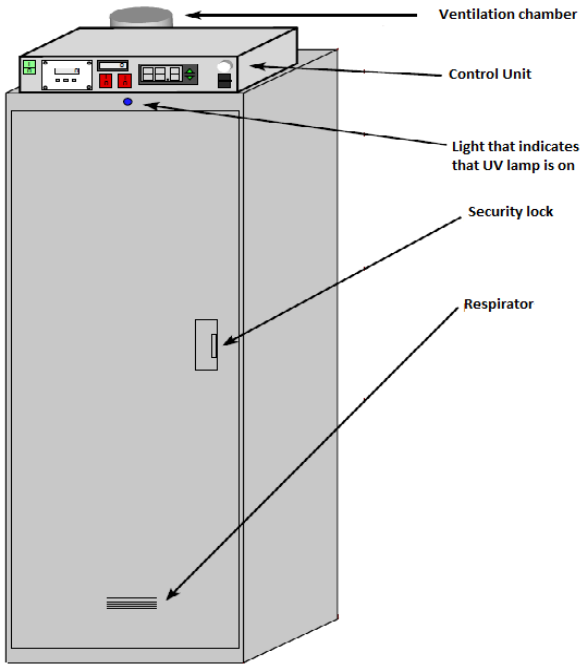

Figure 3.2: Scheme of the ultraviolet system. (Adapted from [26]**).**

When matter is exposed to UV radiation it is subjected to a dose of radiation, D ($W.s/m^2$), which corresponds to a radiant flux (Irradiance), I, multiplied by the exposure time, t (s), as shown in equation 3.1:

$$D = I.t \qquad (3.1)$$

Since irradiance can be defined as the radiant flux (power) received by a surface per unit area, it is expressed in W/m^2. Geometrically as shown in **Figure 3.3**, the irradiance in a point "P" on a small surface, at a distance "a" from an ideal linear radiation source AB of length "l" is given by equation 3.2:

$$I = \frac{\varphi}{2\pi^2 . l . a} * (2\alpha + \sin 2\alpha) \qquad (3.2)$$

Where φ is the total radiation flux (W), and α is given in radian (rad) by equation 3.3:

$$\alpha = arctg(\frac{l}{2.a}) \qquad (3.3)$$

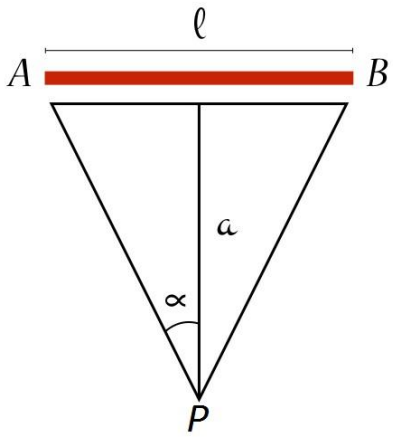

Figure 3.3: Mathematical description of irradiance for an ideal linear radiation source.

For the irradiations that were done in the course of this project, the distance from the source to the samples was 14 cm, with an irradiance of approximately 8 W/m^2.

3.4 Characterization Techniques

3.4.1 Ultraviolet-visible (UV-Vis) and Vacuum Ultraviolet (VUV) spectroscopy

The interaction between molecules and UV radiation can be measured using UV-Vis Spectroscopy. UV radiation and visible light have sufficient energy to promote electrons from the ground state to an excited state [27]. The dissipation of this absorbed energy can occur through chemical changes, emission of light or emission of heat [28].

The electrons involved in simple chemical bonds are designated as σ electrons, while the ones involved in double bonds are called π electrons. In molecules where double bonds are present, π electrons predominate and determine the energy states of the valence electrons. The valence electrons are excited by the absorption of UV or visible radiation. Non-bonding electrons are designated as n electrons [29].

The spectroscopy characterization technique is based on different electronic transitions that are responsible for the spectrum. The peaks observed in the obtained spectrum (absorbance versus wavelength) are centered in the wavelength that corresponds to the necessary energy for the electronic transition to occur. The intensity of the peaks depends on the energy of the molecular orbital and also on the quantic efficiency of the transitions. It is also possible to identify wavelength deviations of the observed peaks to greater or smaller wavelength (bathochromic effect and hypochromic effect respectively) [30].

The electronic transitions can be classified into three different groups, the first one being the one that encompasses transitions from an orbital in its ground state to another one of higher energy, transitions $\pi \rightarrow \pi^*$, and transitions $\sigma \rightarrow \sigma^*$. The second group corresponds to the transitions that occur from a non-bonding atomic orbital to a molecular orbital of higher energy, $n \rightarrow \pi^*$ and $n \rightarrow \sigma^*$. The third group includes transitions from an orbital in its ground state to a Rydberg orbital (higher energy states that converge on an ionic state with an ionization energy) [7]. These transitions and their correspondent region of occurrence in the electromagnetic spectrum are presented in **Table 3.2**.

Transitions in the vacuum ultraviolet (wavelengths below 200 nm) are mainly due to $\sigma \rightarrow \sigma^*$ and to $n \rightarrow \sigma^*$ (**Figure 3.4**). In order to obtain a VUV spectrum, the whole optical path of the spectrometer has to be kept under vacuum [31].

Table 3.2: Electronic transitions associated with regions of the electromagnetic spectrum

Transitions	Region of the electromagnetic spectrum
$\sigma \rightarrow \sigma^*$	Vacuum Ultraviolet
$\pi \rightarrow \pi^*$	Ultraviolet
$n \rightarrow \pi^*$	Near Ultraviolet
$n \rightarrow \sigma^*$	Far Ultraviolet
Rydberg	Vacuum Ultraviolet

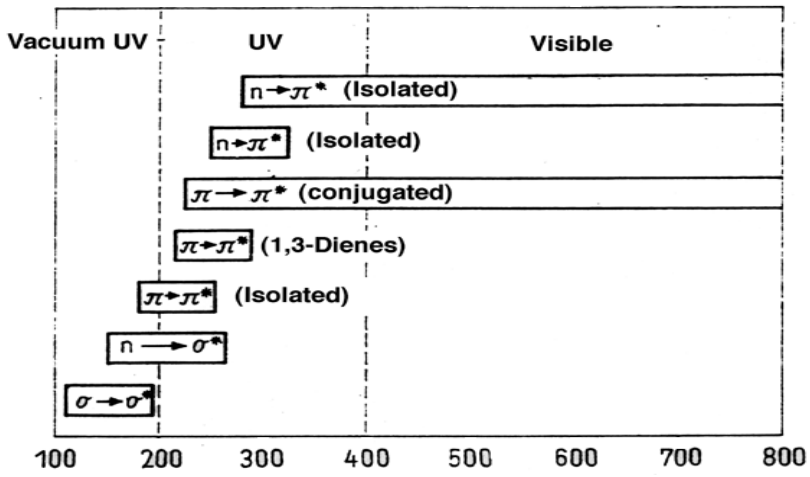

Figure 3.4: Schematic representation of the transitions for each region of the electromagnetic spectrum (Adapted from [31]**).**

UV-Vis spectrophotometers usually contain two light sources: a UV lamp, which emits light in the UV region and a tungsten–halogen lamp for the visible region. After passing through a monochromator (or through optical filters) the light is focused into the cuvette and the amount of light that passes through the sample is detected by a photomultiplier or a photodiode. In double-beam instruments a cuvette with buffer is placed in the reference beam, and its absorbance is subtracted from the absorbance measured for the sample. A schematic diagram of a double-beam spectrophotometer is shown in **Figure 3.5**.

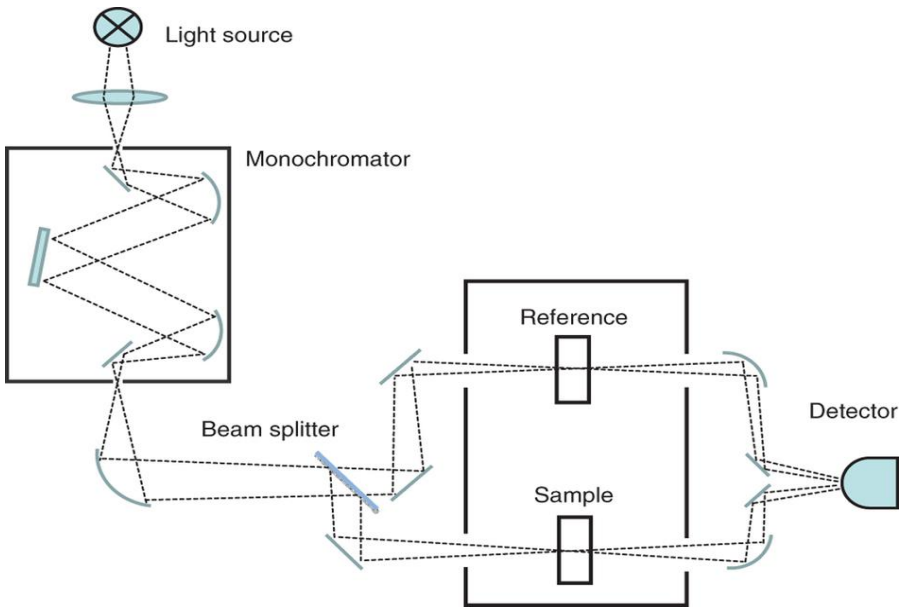

Figure 3.5: Schematic diagram of a double-beam spectrophotometer (Adapted from [32]**).**

Solutions of DNA, 1,10-phenanthroline (Phen), and DNA+Phen, were analyzed by UV-Visible spectroscopy, in sealed quartz cuvettes. The spectra were obtained in the interval of wavelength from 200 nm to 600 nm using the Shimadzu UV-2101PC spectrophotometer.

The VUV spectra presented in this work were recorded at the ultraviolet beam line (UV1) (**Figure 3.6**) in the Synchrotron Radiation facility ASTRID at Aarhus University, Denmark. The setup consists of a sample vacuum chamber containing up to three CaF_2 sample disks and one reference disk mounted on a MDCSBLM-266-4 push-pull linear motion. The VUV beam light passed through the disks and the transmitted intensity was measured at 1.0 nm intervals using a photomultiplier detector (Electron Tubes Ltd., UK). The transmitted light intensity and the synchrotron beam ring current were measured at each wavelength, with a typical resolution better than 0.08 nm. The sample chamber has a LiF entrance window and a MgF2 exit window in front of the photomultiplier. The minimum wavelength is determined by the CaF2 substrates so that the lowest wavelength at which reliable data could be collected was ~ 125 nm. In order to avoid absorption from molecular oxygen in air for wavelengths below 190 nm, the small gap between the sample chamber exit window and the photo multiplier detector was flushed with He gas. To calculate the absorbance, the light intensity spectrum of the CaF_2 disc was measured before and after measuring the spectrum of the cast film. The average of those two spectra and the spectrum of cast film were used to calculate the absorbance using the Beer-Lambert equation. [33].

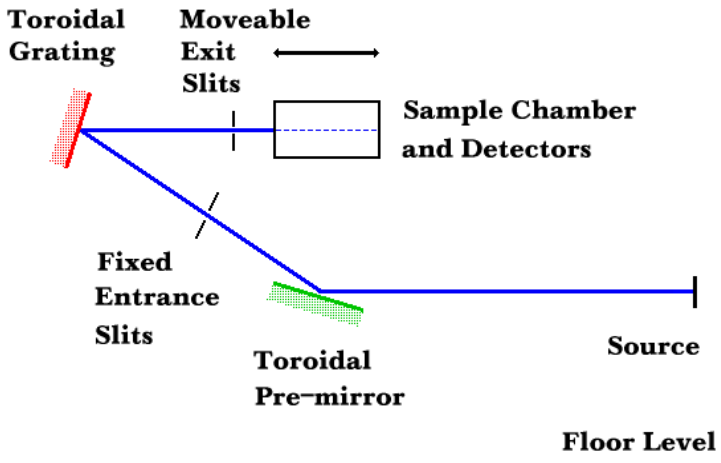

Figure 3.6: Sketch of the ultraviolet beamline (UV1) [34].

3.4.2 Fourier Transform Infrared (FTIR) Spectroscopy

Fourier Transform Infrared (FTIR) is one method of infrared spectroscopy. The FTIR spectrum is obtained in a form of an interferogram which is a plot of the sums of the cosine waves of all the frequencies present in the source of infrared radiation as modified by passage through the sample. These signals are then stored in a computer that carries out Fourier transformations on them, corrects for the frequencies generated by the source of the infrared radiation, and plots the FTIR spectrum [35]. A diagram of a typical FTIR spectrophotometer is shown in **Figure 3.7**.

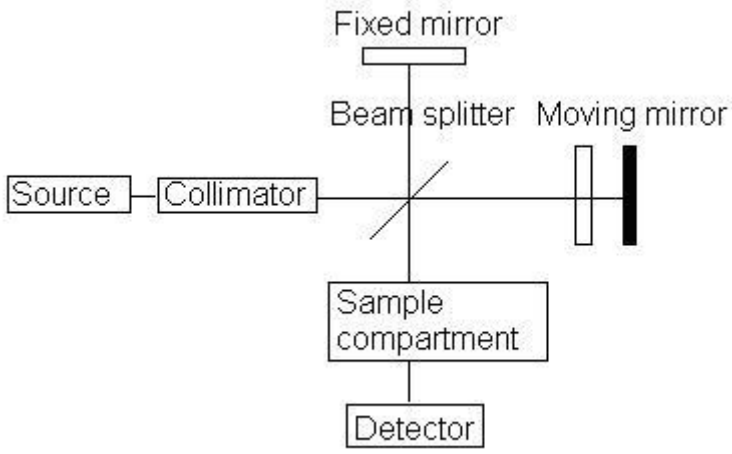

Figure 3.7: Diagram of a FTIR spectrophotometer (Adapted from [36]).

When using infrared (IR) spectroscopy to study a sample, IR radiation passes through, some of which is absorbed by the sample and some of which passes through (is transmitted). Considering that each molecule has its own way of absorbing and transmitting radiation, the resulting spectrum can be considered a molecular fingerprint. Therefore FTIR can be used to determine the identity of unknown materials in a sample, to determine the amounts of components in a mixture, as well as the consistency of a sample [37].

The chemical bonds in a molecule are constantly being distorted because of the motion of its atoms. These motions, designated as molecular vibrations, can be of two types [35]:

- Stretching: there is variability in bond length; it can be either symmetric or antisymmetric.
- Bending: there is variability in bond angle, it can lead to four different types of vibrational modes; scissoring, rocking, twisting, and wagging.

Different vibrational modes are shown in **Figure 3.8**.

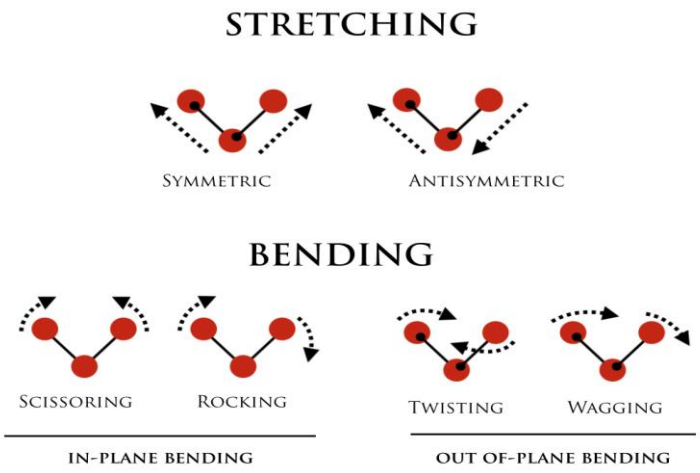

Figure 3.8: Vibrational modes of molecules.

Each molecule has a number of energy levels corresponding to the different vibrational states possible for that molecule. When the radiation impinges the molecule, and its energy is equal to the energy difference between molecular vibrational energy levels, the radiation is absorbed and the amplitude of molecular vibration increases. This absorption is recorded by a FTIR spectrophotometer. Different functional groups absorb at different frequencies, corresponding to certain vibrations typical of that portion of a molecule. The types of bonds present in a molecule determine the frequencies at which functional groups absorb energy, and this is why each molecule has a unique FTIR spectrum [35]. The spectrophotometer Perkin Elmer Spectrum 2000, from the Chemistry Department, FCT-UNL, Lisboa, was used to characterize the produced cast films.

4

Characterization by VUV spectroscopy

The characterization of the DNA lesions caused by UV radiation in the presence of *1,10-phenanthroline* (Phen) is presented in this chapter. The characterization was obtained by vacuum ultraviolet (VUV) spectroscopy of cast films prepared with aqueous solutions of DNA, Phen, and DNA+Phen. The software *OriginPro 9.0*, was used for graphing and analyzing the obtained data.

4.1 Characterization of the solutions of DNA, and 1,10-phenanthroline

VUV absorption measurements were made in order to characterize the interaction between DNA and the intercalator 1,10-phenantthroline. The obtained spectra were adapted by Gaussian curves with the aim of improving the characterization of the obtained peaks.

Figures 4.1 depicts the VUV absorption spectrum of 1,10-phenanthroline. In order to attribute the electronic transitions to the respective band, an extensive research of the known constituents of Phen was made, namely pyrimidine and benzene. This information is listed in **Table 4.1.**

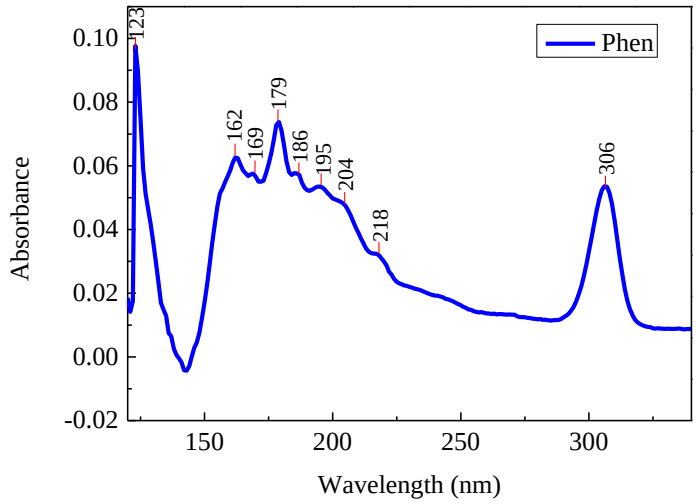

Figure 4.1: VUV absorption spectrum of 1,10-phenanthroline.

Table 4.1: Peak parameters for VUV data of Phen.

Peak position (nm)/(eV)	Electronic Transition	Structure	Functional Group
162/7.65	-		Pyridine [38]
169/7.34	-		Benzene Band $^1E_{1u}$ (7.0 eV) [39]
179/6.93	$\pi \rightarrow \pi^*$		Pyridine [38]
186/6.67	$\pi \rightarrow \pi^*$		Pyridine [38]
195/6.35	$\pi \rightarrow \pi^*$		Benzene Band $^1B_{1u}$ (6.2eV) [38]
205/6.08	$\pi \rightarrow \pi^*$		Pyridine [38]
218/5.89	$n \rightarrow \pi^*$		Pyridine ($^1A_2$) [38]
306/4.05	-	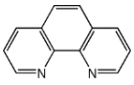	Conjugation

4.2 The effect of UV radiation

The prepared cast films were irradiated at a fixed wavelength (140 nm) for three hours under vacuum, in order to study the effect of UV radiation on the degradation of the molecules. The obtained spectra before and after irradiation, are shown in **Figure 4.2** for DNA+1,10-phenanthroline.

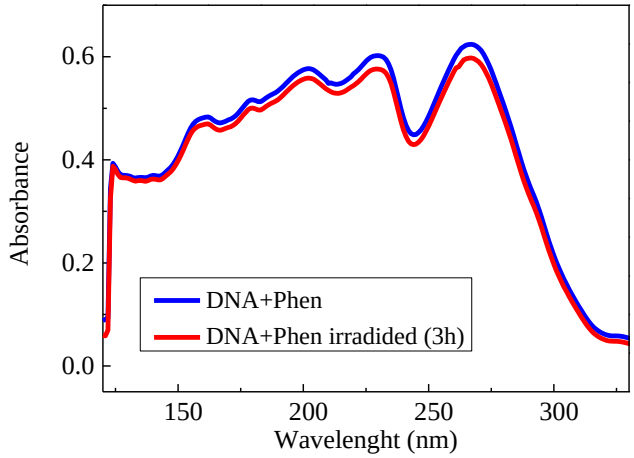

Figure 4.2: VUV absorption spectra of cast films of DNA+Phen, before and after being irradiated for a period of 3 hours.

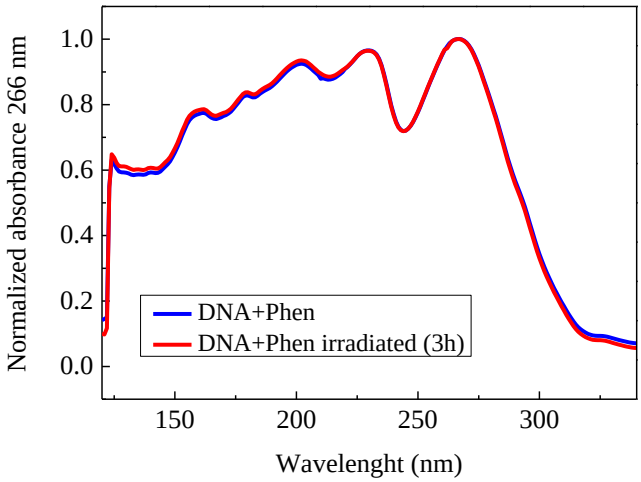

Figure 4.3: VUV normalized absorption spectra of cast films of DNA+Phen, before and after being irradiated for a period of 3 hours.

Considering **Figure 4.1** we can observe that there is little change in the spectrum obtained after irradiation. The difference between the two spectra, obtained before and after irradiation, becomes less significant when the absorption spectra are normalized to the peak at 266 nm (**Figure 4.2**). These results corroborate the results of Gomes [40], that show that in the absence of water the samples are not affected by the exposure to UV radiation. Therefore, VUV characterization is a useful technique to characterize the materials, but we will have to resort to other characterization techniques in order to study the effect of UV radiation on DNA in the presence of the intercalator.

4.3 Conclusions

Cast films of 1,10-phenanthroline, and DNA+1,10-phenanthroline, were characterized by VUV spectroscopy, and the electronic transitions were assigned for each band present in the obtained spectra.

There was no significant change in the spectra obtained after the irradiation of the samples under vacuum, which leads to the conclusion that the presence of water is essential in order to observe the effect of UV radiation.

5

Effect of UV radiation- characterization by UV-Vis

The characterization of the DNA lesions caused by UV radiation in the presence of *1,10-phenanthroline*, is presented in this chapter. The characterization was obtained by UV absorption spectroscopy of aqueous solutions of DNA, *1,10-phenanthroline*, and DNA + *1,10-phenanthroline*. The software *OriginPro 9.0*, was used for graphing and analyzing the obtained data.

5.1 Calculation of the absorption coefficient

The absorption coefficient can be determined using Lambert-Beer's law (**Equation 5.1**), which relates the attenuation of light to the properties of the material through which the light is traveling.

$$A = \log_{10} \frac{I_0}{I} \qquad (5.1)$$

where A, the absorbance, is defined by the incident intensity I_0, and the transmitted intensity I.

Considering that the absorbance is directly proportional to the concentration of the solution of the sample, and that it is also directly proportional to the length of the light path (d) which is equal to the width of the cuvette

$$Abs = \varepsilon dC \qquad (5.2)$$

where Abs is absorbance at a specific wavelength, ε is the absorption coefficient, d is the thickness of the cuvette, and C is the concentration of the solution. Once the absorption coefficient is

known, the expected absorbance value for a known concentration can be calculated using equation 5.1.

In order to calculate the absorption coefficient of 1,10-phenanthroline (Phen), solutions with different concentrations were prepared from an inicial solution of Phen with a concentration of 20 µM. **Figure 5.1** shows the UV-Vis absorbance spectra obtained.

Since Phen has two characteristic bands, one at 229 nm, and one at 262 nm aproximately, the values of absorbance at these wavelengths are represented grafically as a function of concentration in **Figure 5.2.** The wavelength of 260 nm was also considered since DNA absorbs at this wavelength.

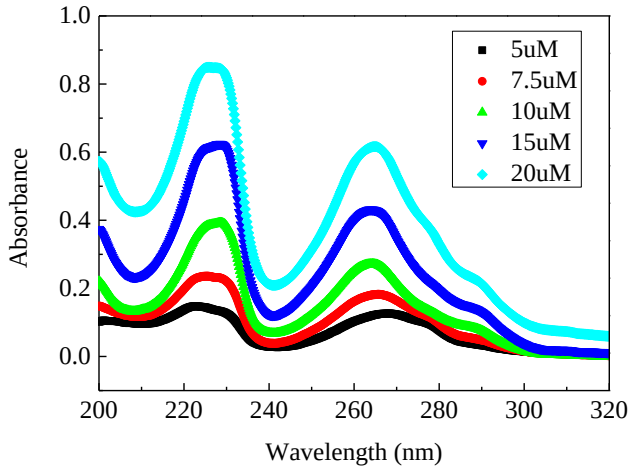

Figure 5.1: UV-Vis absorbance spectra of aqueous solutions of Phen with different concentrations.

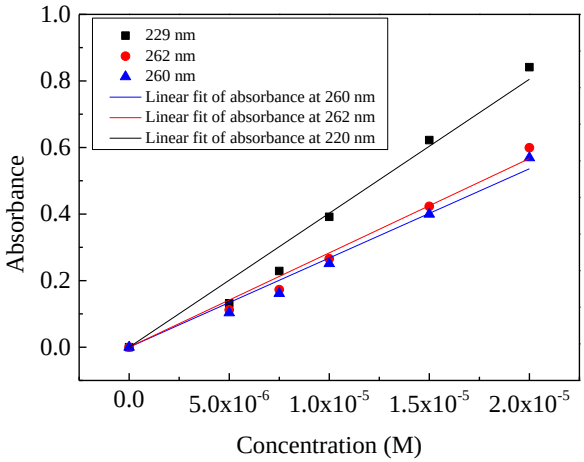

Figure 5.2: Representation of absorbance at different wavelengths as a function of concentration of Phen.

The absorption coefficients were calculated from the slopes obtained from the straight lines which can be put in the form of equation 1, since the thickness of the cuvette is 1 cm. The results for the molar attenuation coefficient at different wavelengths are shown in **Table 5.1.**

Table 5.1: Parameters obtained from the linear fit of absorbance at 229 nm, and 262 nm, where ε is the absorption coefficient of Phen, and R is the correlation coefficient.

Wavelength (nm)	*Slope (dm^3/mol)*	*ε (m^2/mol)*	*Slope (dm^3/g)*	*ε (m^2/g)*	*R*
229	40000±2000	4000±200	240±14	24±1.4	0.99545
262	28000±1000	2800±100	160±8	16±0.8	0.99705

Coelho [41], studied the molar attenuation coefficients for the characteristic peaks of DNA (**Table 5.2**).

Table 5.2: Absorption coefficient of DNA [41]**.**

Wavelength (nm)	*Slope (dm^3/g)*	*ε (m^2/g)*	*R*
230	6,6 ± 0,3	0.66	0,98706
260	15,4 ± 0,8	0.154	0,97767
280	8,5 ± 0,5	0.85	0,96938

5.2 Characterization of the solutions of DNA and 1,10-phenanthroline

In order to study the interaction between DNA and *1,10-phenanthroline* (Phen), firstly the UV-Visible absorption spectra of DNA, Phen, and [1:1](v/v) DNA+Phen were obtained as shown in **Figures 5.3 a), b) and c)** respectively. The obtained spectra were adapted by Gaussian curves with the aim of improving the characterization of the obtained peaks.

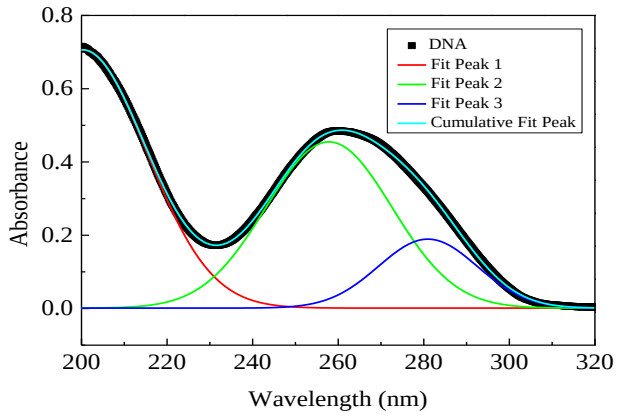

a)

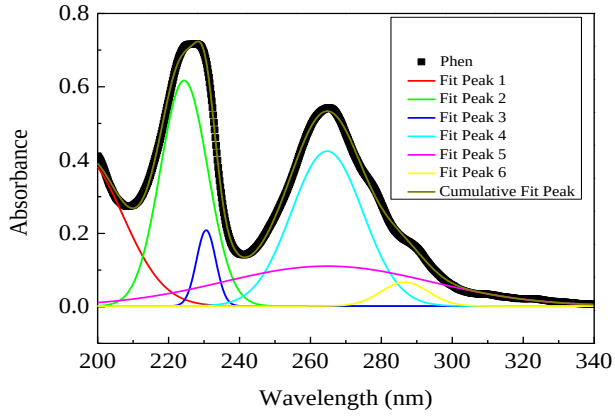

b)

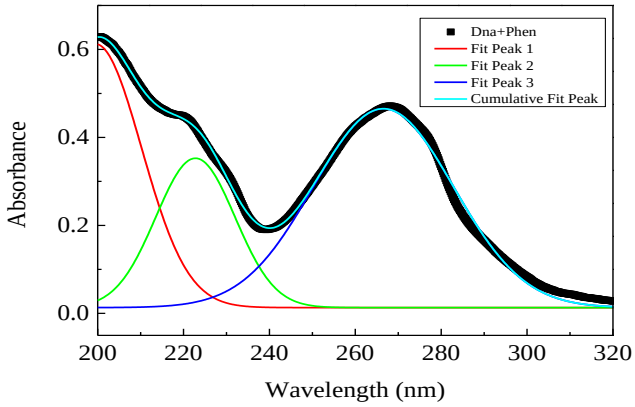

c)

Figure 5.3: UV-Vis absorption spectra of a) DNA, b) 1,10-phenanthroline and c) [1:1](v/v) DNA+1,10-phenanthrolin

Figure 5.3 a) represents the absorption spectrum in the UV/Vis region of an aqueous solution of DNA with a concentration of 0,025 mg/mL. There are two characteristic bands that can be identified in the spectrum of the DNA solution, one at 260 nm, and another at 200 nm approximately**.** The absorption band at 260 nm is, according to literature, attributed to all the DNA bases [42].

The band that is centered at 200 nm can be attributed to the adenine band at 207 nm, or could also be related to the electronic transitions of guanine from $n \rightarrow \pi*$ (209 nm), and of thymine from $\pi \rightarrow \pi*$ (208 nm). The band at 280 nm is associated with $\pi \rightarrow \pi*$ transitions of the DNA [43][44].

The bands and their respective transitions are represented in **Table 5.3.** The spectrum peak structure was obtained by fitting the experimental UV-Vis sprectum with a set of Gaussians.

Table 5.3: Peak parameters obtained from fitting the UV-Vis spectra of DNA and 1,10-phenantroline.

Peak parameters for UV-Vis data of DNA solution		
Peak position (nm)	FWHM (nm)	Assignment
200.26±0.04	35.27±0.09	$n \rightarrow \pi*$ guanine [43] $\pi \rightarrow \pi*$ thymine [43]
257.8±0.1	34.7±0.2	All bases [42]
280.9±0.1	27.2±0.2	$\pi \rightarrow \pi*$ [8]
Peak parameters for UV-Vis data of Phen solution		
Peak position (nm)	FWHM (nm)	Assignment
195±1	27±2	$\pi \rightarrow \pi*$ [45]
224.39±0.09	15.7±2	$\pi \rightarrow \pi*$ [45]
230.60±0.04	6.4±0.1	$\pi \rightarrow \pi*$ [46]
264.71±0.05	23.8±0,3	$\pi \rightarrow \pi*$ [46]
265±1	69±3	$\pi \rightarrow \pi*$ [45]
286.6±0.3	15.7±0.7	

The absorbance spectrum of a 1,10-phenanthroline aqueous solution is shown in **Figure 5.3 b)**. The spectrum presents two main bands, one at 231 nm, and another at 264 nm aproximetly. The results are in agreement with the literature which defines two absorbance maxima, one at 229 nm, and one at 262 nm. These absorption bands are assigned to $\pi \rightarrow \pi*$ transitions of the aromatic ring of 1,10-phenanthroline [46]. The spectrum was devonvoluted into a set of Gaussians in order to obtain more information of each band, which is listed in **Table 5.3.**

5.3 The effect of UV radiation

In order to study the effect of UV radiation, aqueous solutions of DNA, Phen and [1:1](v/v) DNA+Phen were irradiated for different time periods. **Figures 5.4 a)**, **b)** and **c)** represent the absorption spectra obtained before and after each irradiation period for DNA, Phen, and [1:1](v/v) DNA+Phen respectively.

As the irradiation time increases there is an apparent increase of absorbance, which is due to an increase in the baseline absorption. These changes in the baseline upon fragmentation might be indicative of fragmentation [44].

From an analysis of the absorbance spectra is possible to observe the hypochromic effect on the three solutions as the irradiation time period increases. There is a decrease in the intensity of absorbance, which indicating that the molecules in the solutions degrade as the exposure to UV radiation increases. Therefore, we can conclude that UV radiation is able to degrade both molecules, DNA and Phen.

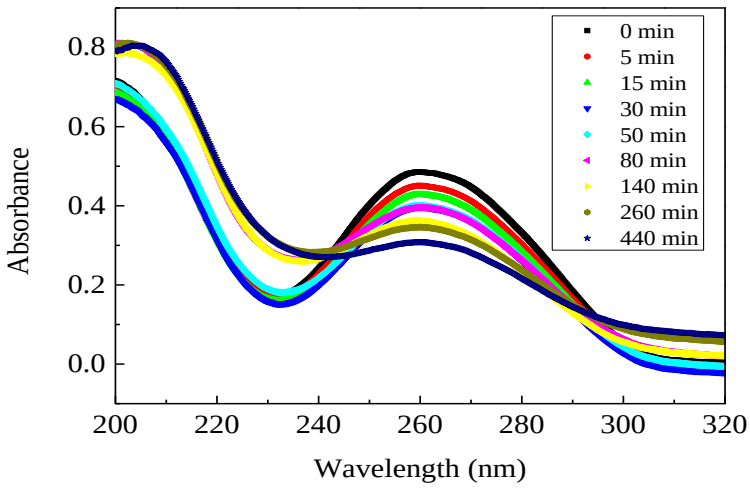

a)

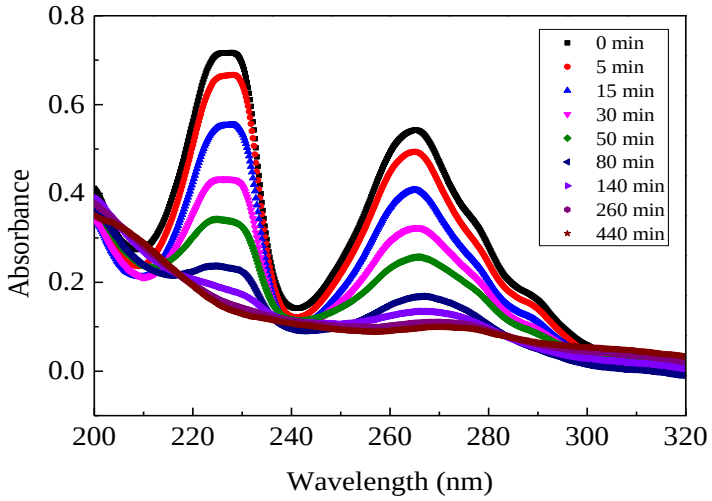

b)

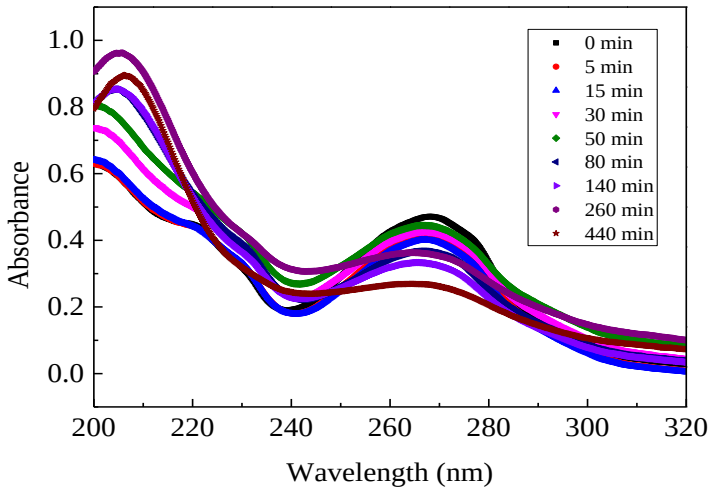

c)

Figures 5.4: Absorbance spectra of a) DNA, b) 1,10-phenanthroline and c) [1:1](v/v)DNA+1,10-phenanthroline, as the time of exposure to UV radiation increases.

In order to analyze the damage caused by UV radiation the characteristic band of DNA, at 260 nm, which is associated with the nitrogenous bases of DNA, was studied. **Figure 5.5** shows the spectra for the 260 nm band, where the normalized absorbance was plotted versus irradiation time.

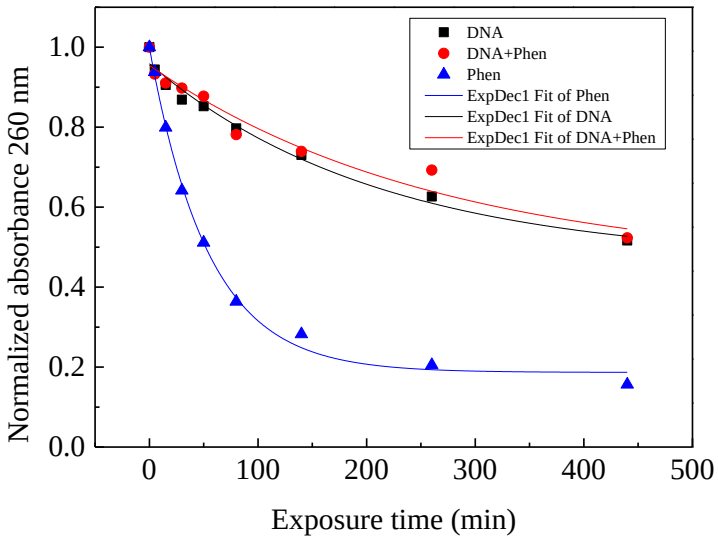

Figure 5.5: Evolution of the normalized absorbance of the band at 260 nm, as the exposure to UV radiation increases for the three different solutions od DNA, Phen, and [1:1](v/v) DNA+Phen.

The exponential time constants for each of the solutions are obtained by doing an exponential fit to the results presented in **Figures 5.4**, in order to analyze the decay for the band at 260 nm. **Table 5.4** shows the data obtained from the fitting.

Table 5.4: Exponential time constant obtained from an exponential fit to the experimental results of the spectra at 260 nm.

	$T_{260\ nm}$ *(min)*
DNA	140±30
DNA+Phen	180±80
Phen	37±2

Analyzing the results listed in **Table 5.4**, we can observe that the DNA solution decays in 140±30 minutes, while in the presence of Phen the decaying time is 180±80 minutes. Considering the fact that the band at 260 nm is associated with the nitrogenous bases of DNA, it can be concluded that the presence of Phen has no major effect on the degradation of the DNA bases. On the other hand the Phen solution decays in 37±2 minutes, which leads to the conclusion that the DNA molecule protects the Phen molecule.

The characteristic bands of Phen (**Figure 5.4 b)**) goes through a much accentuated decrease in absorbance at 230 nm, and 264 nm, which indicates that UV radiation has a significant effect on the degradation of this molecule. It is also possible to observe the bathochromic shift on **Figure 5.4 c)** which confirms the intercalation between DNA and Phen.

In order to analyze the process of degradation of DNA, Phen, and DNA+Phen, some calculations were made, and the results are presented in **Table 5.5** and **5.6**. From these results it is possible to observe that the expected absorbance for the three solutions has approximately the same value as the obtained absorbance, after being irradiated for 30 minutes. This information shows us that these processes of degradation are independent of one another, meaning that what happens in one molecule does not affect what happens in the other molecule.

Table 5.5: Calculations of Abs_{260} taking into account the initial concentration of the samples.

Solutions	DNA concentration (mg/mL)	Expected DNA Abs_{260} [41]	Phen concentration (M)	Expected Phen Abs_{260}[a]	Expected Abs_{260}	Obtained Abs_{260}
DNA	0.025	0.385	0	0	0.385	0,485
Phen	0	0	$2*10^{-5}$	0.53606	0.53606	0,4919
DNA+Phen	0.0125	0.1925	$1*10^{-5}$	0.26803	0.46053	0.4254

[a]From Figure 5.2

Table 5.6: Abs_{260} after being irradiated for 30 minutes.

Solutions	Abs_{260} (t= 0 mn)	Calculated Abs_{260} (t= 30 mn)[a]	Obtained Abs_{260} (t= 30 mn)
DNA	1	0.8937	0.8688
Phen	1	0.6537	0.6419
DNA+Phen	1	0.8977	0.8977

[a]From Figure 5.5

5.4 Conclusions

The aqueous solutions of DNA, Phen, and DNA+Phen were characterized by UV-Vis spectroscopy. The obtained characteristic band for each solution were attributed the correspondent electronic transition. The evolution of the absorbance at 260 nm, as the irradiation time increased was analyzed. Both DNA and Phen molecules are degraded by UV radiation, however, the presence of the intercalator has no effect on the degradation of the DNA bases. The degradation processes happen by independent processes.

6

Effect of UV radiation- characterization by FTIR

In this chapter the damage caused by UV radiation on DNA in the presence of the intercalator 1,10-phenanthroline, is characterized by Fourier transform infrared spectroscopy (FTIR). Cast films were prepared with solutions of DNA, Phen, and DNA+Phen, which were irradiated for different time intervals. The software *OriginPro 9.0*, was used for graphing and analyzing the obtained data.

6.1 Characterization of DNA and Phen

Cast films of the solutions of DNA, and DNA+Phen, were characterized by FTIR.

Figures 6.1 a) and **b)** represent the obtained absorbance spectra for DNA, Phen and DNA+Phen respectively, from 900 to 1800 cm^{-1}.

The main components of DNA, namely, sugars, bases and phosphates, can be identified in **Figure 6.1 a)**. **Tables 6.1** and **6.2** list the spectral assignments of DNA and Phen respectively.

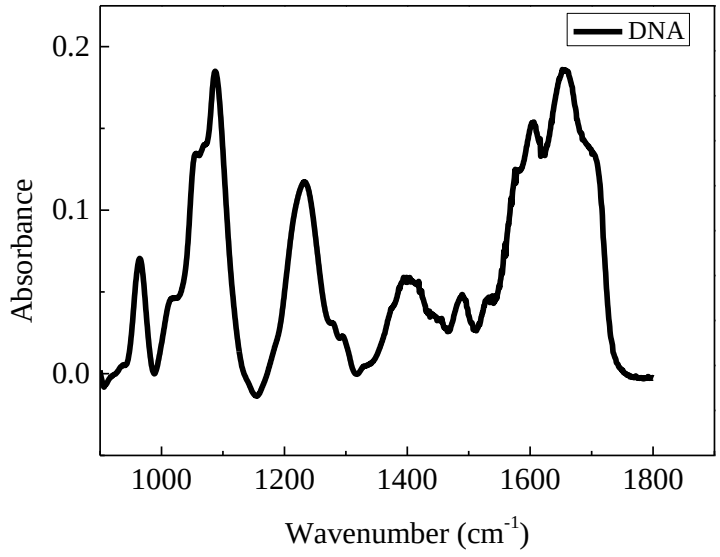

a)

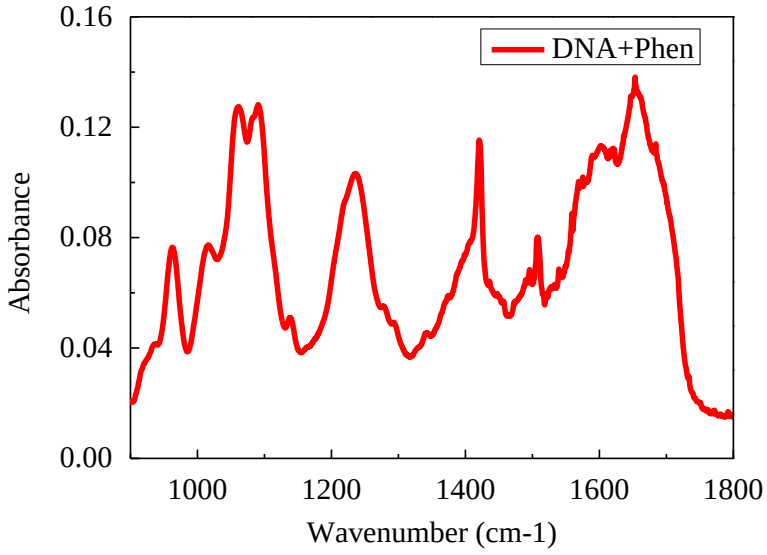

b)

Figure 6.1: Infrared absorbance spectrum of a) DNA, and b) DNA+Phen.

Table 6.1: Characteristic infrared absorptions in DNA cast films [47]**.**

Wavenumber ***(cm^{-1})***	***Literature wavenumber*** ***(cm^{-1})***	***Assignment***
965	950-970	CC stretch of the backbone
1015	1010-1020	Furanose Vibrations
1055	1044-1069	CO stretch of the furanose backbone
1087	1085-1090	Symmetric PO_2^- stretching of the backbone
1232	1235-1245	Antisymmetric PO_2^-stretch in A-form
1280	1281 1275	C5=C6 vibration of cytidine CN3H bend of deoxyribose thymine
1295	1285-1297	C4-NH2 strength of cytosine
1393	1374-1389 1369-1381	CH_3 Symmetric deformation of deoxyribose thymine Cytidine and guanosine in anti-conformation
1575	1575-1590	C=N ring vibration of Guanine single stranded or double stranded
1604	1601	C=N ring vibration of guanine
1657	1655-1657	C2=O2 strength of cytosine single stranded or double stranded
1701	1691-1698	C2=O2 strength of thymine single stranded or double stranded
1716	1712 1715	Stretching of thymines involved in reverse Hoogsteen third strand binding. C6=O6 stretching of guanines involved in Hoogsteen third strand binding and/or C2=O2.

Table 6.2: Characteristic infrared absorptions in Phen cast films and their assignment [48][49][50]**.**

Wavenumber (cm^{-1})	**Assignment**
854	Benzene ring bending
988	Ring breathing
1092	CCC bending in-plane
1139	CCC bending in-lane and HCC bending in-plane
1217	HCC bending in-plane
1344	CN stretching, CC stretching, and HCC bending in-plane
1421	CC stretching, and HCC bending in-plane
1505	HCC bending in-plane
1588	CC stretching, and HCC bending in-plane
1643	CC stretching

6.2 Characterization of the effect of UV radiation

The evolution of the infrared absorption spectra of DNA, and [1:1](v/v) DNA+Phen is represented in **Figures 6.2 a)**, and **b)** respectively, from 900 to 1800 cm^{-1}. The cast films were prepared with aqueous solutions and exposed to UV radiation for different periods of time.

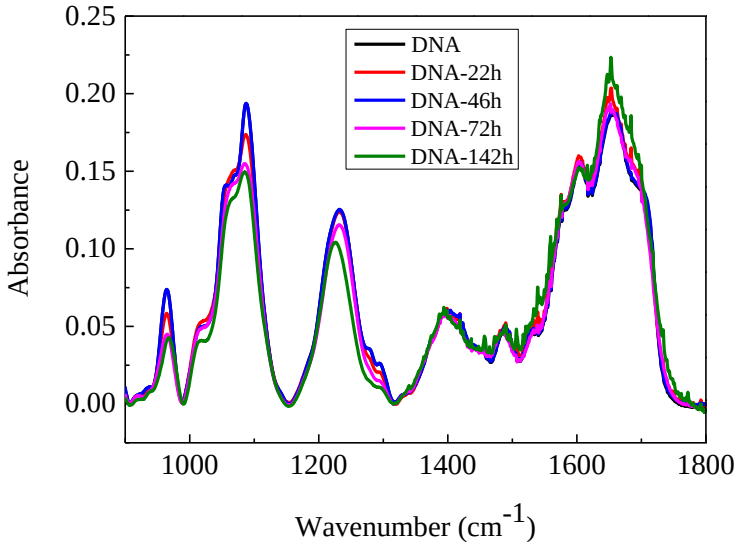

a)

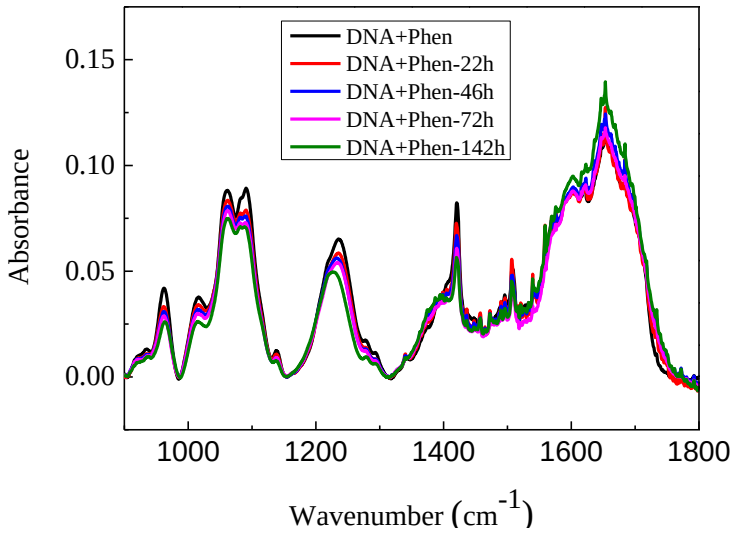

b)

Figure 6.2: Infrared absorbance spectra of a) DNA and b) DNA+Phen cast samples exposed to different intervals of irradiation.

In order to analyze the obtained results, the baseline was subtracted from the spectra. To simplify the analysis, the spectra were divided into different regions, from 900 to 1400 cm^{-1} and from 1400 to 1800 cm^{-1}.

The evolution of the infrared absorbance spectra of DNA and [1:1](v/v) DNA+Phen, in the first interval, from 900 to 1400 cm^{-1}, is represented in **Figures 6.3 a)** and **b)** respectively.

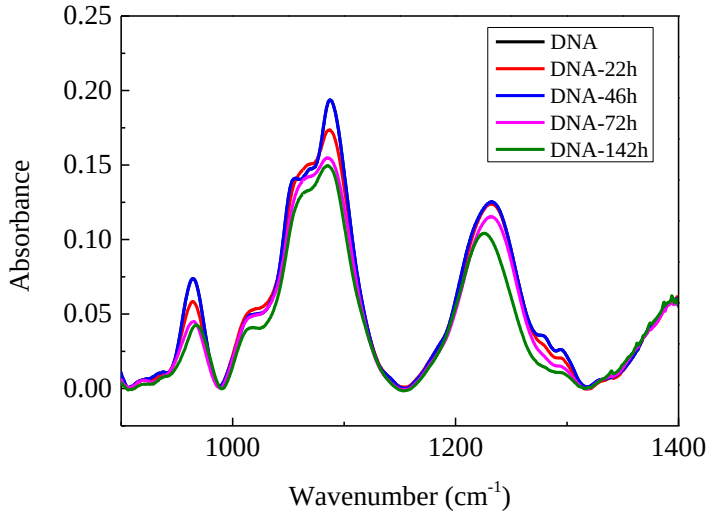

a)

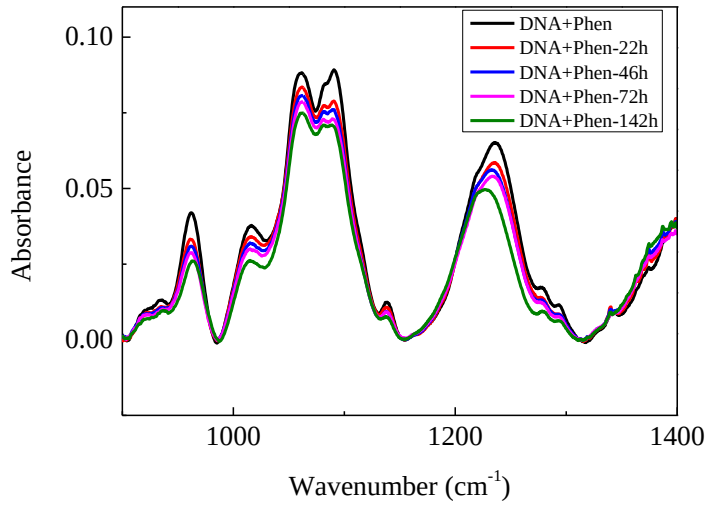

b)

Figure 6.3: Infrared absorbance spectra, , from 900 cm^{-1} to 1400 cm^{-1} of a) DNA and b) DNA+Phen cast samples exposed to UV radiation for different periods of time.

Figures 6.3 a) and **b)** show that the damage caused on the DNA molecule, occurs at the sugars and phosphate groups. In order to analyze in more detail the damage caused on DNA when exposed to UV radiation in the presence of Phen, the evolution of each characteristic peak is studied.

Figures 6.4 a) and **b)** represent the evolution of the peak at 965 cm^{-1} for DNA and [1:1](v/v) DNA+Phen respectively. These figures show that the absorbance decreases as the time that the cast film is exposed to UV radiation increases. Since the peak at 965 cm^{-1}, is identified in the literature as being associated with the CC stretch of the backbone [44], and therefore related to the vibration of the sugar ring, it can be concluded that the wavelength of 254 nm is enough to break the sugar ring.

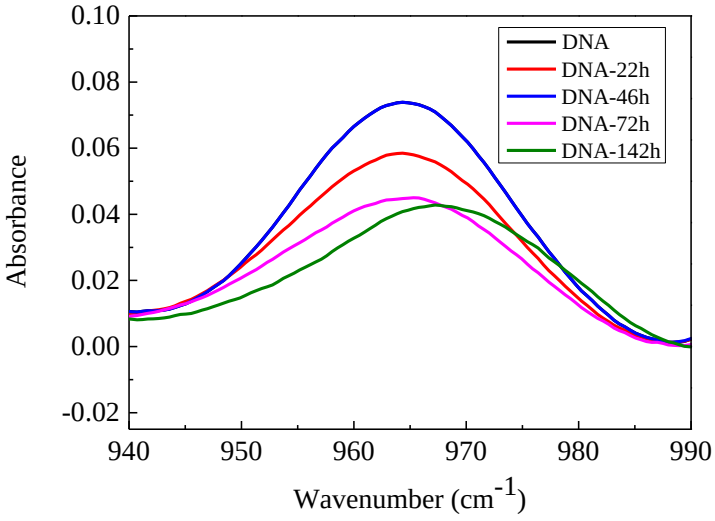

a)

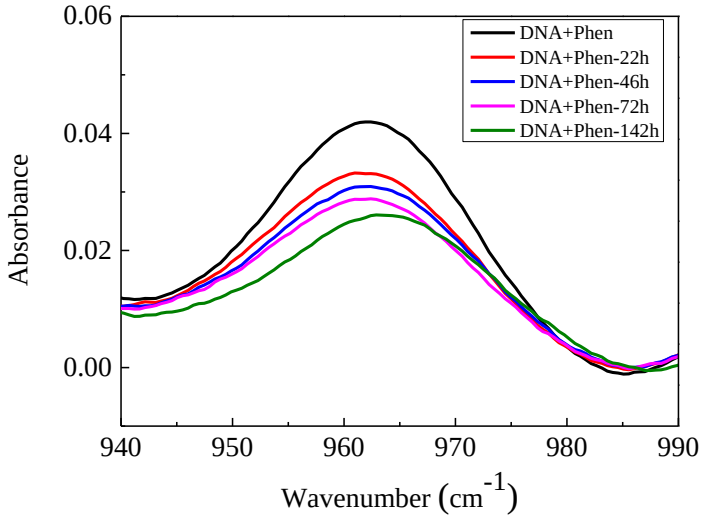

b)

Figure 6.4: Evolution of the peak at 965 cm^{-1}, of the infrared absorbance spectra of DNA+Phen cast film irradiated for different time periods.

The exponential time constants for each of the solutions are obtained by doing an exponential fit (**Figure 6.5**) to the results presented in **Figures 6.4 a)**, and **b)** in order to analyze the evolution of this peak (965 cm^{-1}).

The presence of the intercalator Phen has a protective effect on the degradation of the DNA molecule for this particular peak. The DNA molecule decays in 137±27 hours, while in the presence of Phen the decaying constant is 175±43 hours.

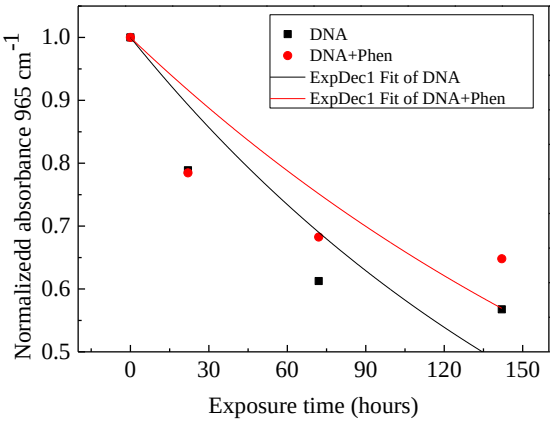

Figure 6.5: Evolution of the peak at 965 cm^{-1}, of the infrared absorbance spectra of DNA and DNA+Phen cast film as the exposure time to UV radiation increases.

Figures 6.6 a) and **b)** represent the infrared absorbance spectra of DNA and DNA+Phen respectively, from 1000 to 1150 cm^{-1}. From **Figure 6.6 a)** it is possible to observe that the peak at approximately 1015 cm^{-1}, which is assigned to furanose vibrations, does not go through a significant absorbance variation as the sample is exposed to UV radiation, which makes it possible to infer that UV radiation does not lead to alterations on this DNA component. However, in the presence of Phen (**Figure 6.6 b)**) there is a decrease of absorbance as the irradiation time increases. **Table 6.3** lists the results of an exponential fitting (**Figure 6.7**) of the normalized absorbance at 1015 cm^{-1}, as the exposure time to UV radiation increases.

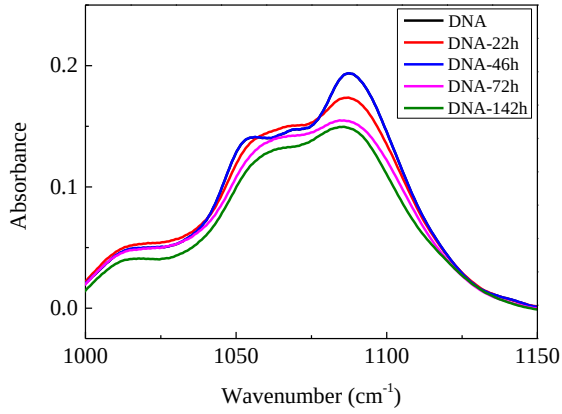

a)

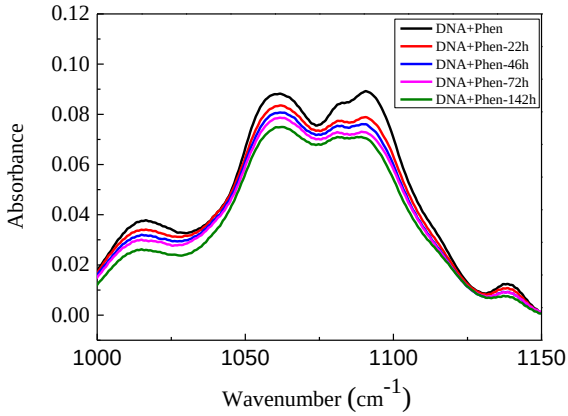

b)

Figure 6.6: Infrared absorbance spectra of a) DNA, and b) DNA+Phen cast films irradiated for different time periods, from 1000 to 1150 cm^{-1}.

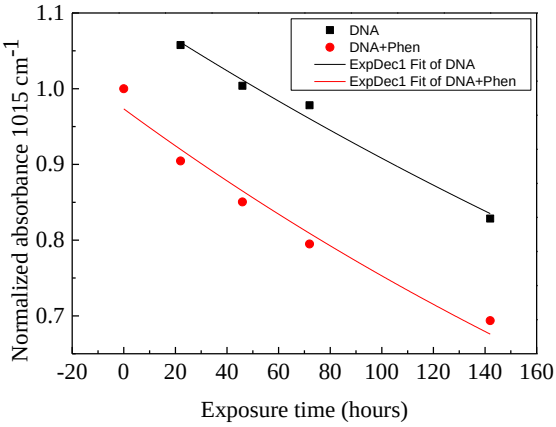

Figure 6.7: Evolution of the peak at 1015 cm^{-1}, of the infrared absorbance spectra of DNA and DNA+Phen cast film as the exposure time to UV radiation increases.

Considering the peaks at 1055 and 1087 cm^{-1}, shown in **Figures 6.6 a)** and **b)** it is clear that there is a decrease in the absorbance value at these wavelengths as the irradiation time increases. These peaks are assigned to the CO stretch of the furanose backbone (1055 cm^{-1}), and to the symmetric PO_2^- stretching of the backbone (1087 cm^{-1}).

Figure 6.8 shows the exponential fitting of the normalized absorbance at 1055 cm^{-1}. From the information listed on **Table 6.3**, it is possible to infer that in the presence of Phen, the peak at 1055 cm^{-1}, which is assigned to the CO stretch of the furanose backbone, decays more rapidly.

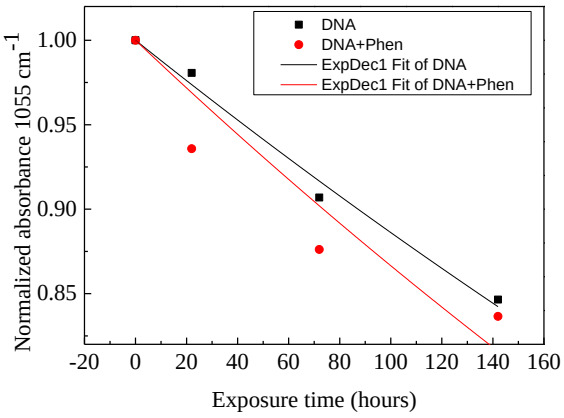

Figure 6.8: Evolution of the peak at 1055 cm^{-1}, of the infrared absorbance spectra of DNA and DNA+Phen cast film as the exposure time to UV radiation increases.

DNA irradiation leads to an exponential decay of the phosphate groups [44], which is represented in **Figure 6.9**. From the information listed on **Table 6.3** it is not possible to conclude about the effect of Phen on the peak at 1087 cm^{-1}, which refers to the symmetric PO_2^- stretching of the backbone, due to the error present.

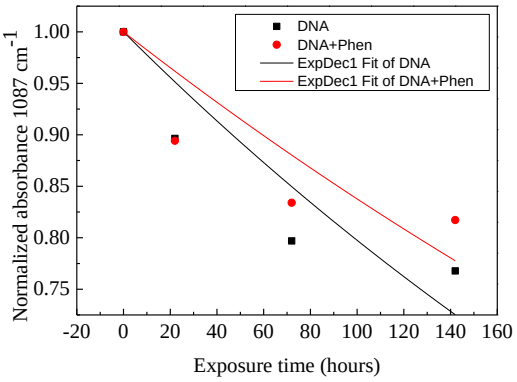

Figure 6.9: Evolution of the peak at 1087 cm^{-1}, of the infrared absorbance spectra of DNA and DNA+Phen cast film as the exposure time to UV radiation increases.

Figures 6.10 a) and **b)** represent the infrared spectra of DNA and DNA+Phen respectively, from 1150 to 1300 cm^{-1}.

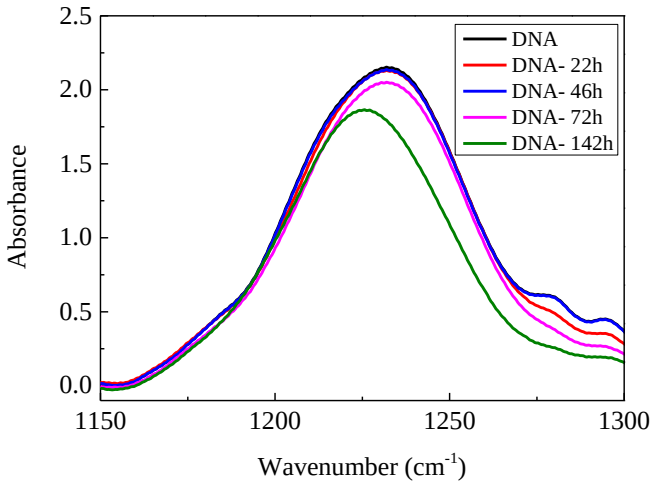

a)

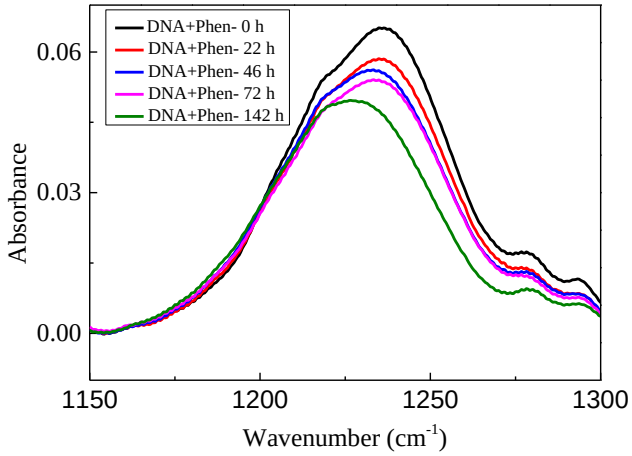

b)

Figure 6.10: Infrared absorbance spectra of a) DNA and b) DNA+Phen cast films irradiated for different time periods, from 1150 to 1300 cm^{-1}.

In order to analyze the evolution of the peak at 1232 cm^{-1}, which is assigned to the anti-symmetric PO_2^- stretch in A-form, the exponential time constants for each of the solutions are obtained by doing an exponential fit (**Figure 6.11**) to the results presented in **Figures 6.10 a)**, and **b)**. These results show that as mentioned before, exposure to UV radiation leads to loss of

the phosphate groups. In the presence of Phen, the degradation is more accentuated and there is an exponential decay. It was not possible to infer about the effect of Phen on the degradation of DNA because it was not possible to do an exponential fitting to the results of the DNA solution.

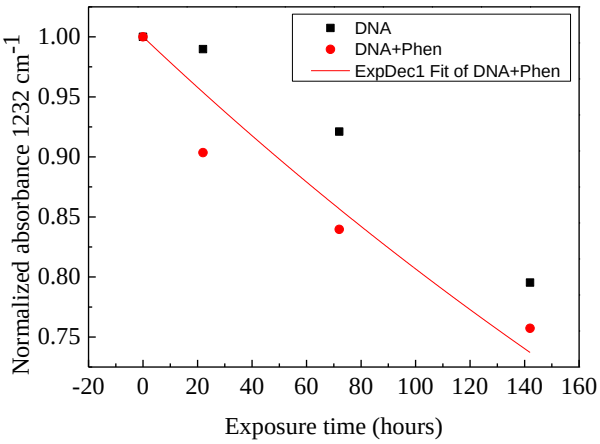

Figure 6.11: Evolution of the peak at 1232 cm^{-1}, of the infrared absorbance spectra of DNA and DNA+Phen cast film as the exposure time to UV radiation increases.

From **Figures 6.10 a)** and **b)** it is also possible to obtain information about the peaks at 1280 and 1295 cm^{-1}, which refer to the C5=C6 vibration of cytidine, or to the CN3H bend of deoxyribose thymine, and to the C4-NH2 strength of cytosine respectively. The decaying constants for each of the solutions are obtained by doing an exponential fit in order to analyze the evolution of the peak at 1280 cm^{-1} (**Figure 6.12**), and of the peak at 1295 cm^{-1} (**Figure 6.13**). The obtained results (**Table 6.3**) show that for both peaks the degradation occurs more rapidly in the absence of the intercalator, with Phen acting as a protective agent.

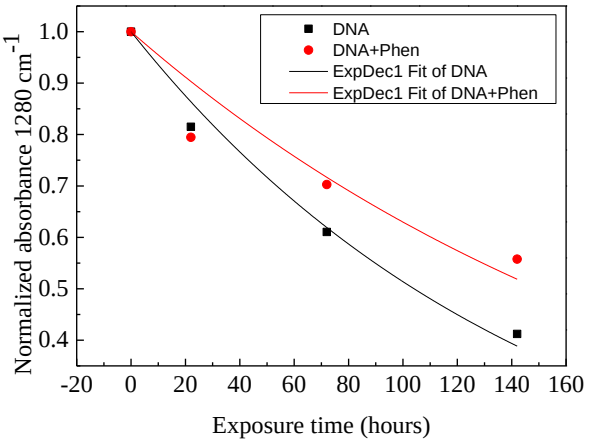

Figure 6.12: Evolution of the peak at 1280 cm^{-1}, of the infrared absorbance spectra of DNA and DNA+Phen cast film as the exposure time to UV radiation increases.

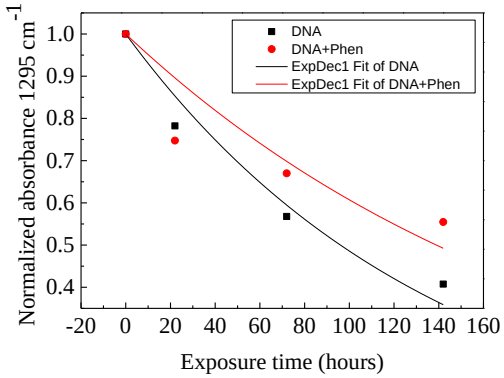

Figure 6.13: Evolution of the peak at 1295 cm^{-1}, of the infrared absorbance spectra of DNA and DNA+Phen cast film as the exposure time to UV radiation increases.

Figures 6.14 a) and **b)** show the evolution of the spectra of DNA and DNA+Phen respectively, from 1300 cm^{-1} to 1400 cm^{-1}, as the irradiation time increases.

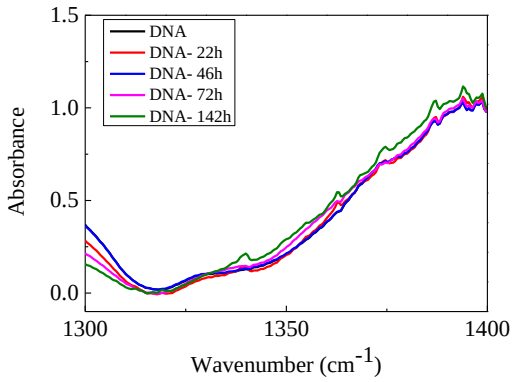

a)

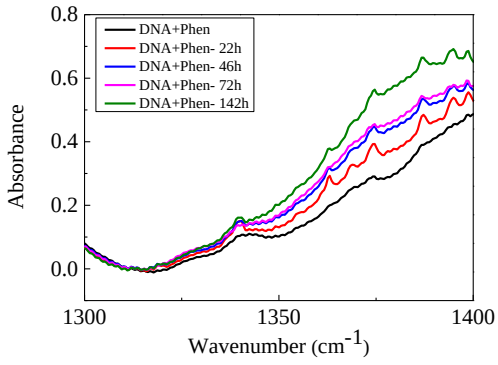

b)

Figure 6.14: Evolution of the absorbance spectra of a) DNA and b) DNA+Phen, from 1300 to 1400 cm^{-1}, as the irradiation time increases.

Figures 6.15 a) and **b)** represent the infrared absorbance spectra of DNA and DNA+Phen respectively, from 1400 to 1800 cm^{-1}. This particular region is related to the DNA bases. Even though there is a considerable amount of noise present in the spectra in this particular region, it is possible to see the evolution of the peaks at around 1604 cm^{-1}, and 1653 cm^{-1}. These peaks are assigned to the C=N ring vibration of guanine, and to the C2=O2 strength of cytosine single stranded or double stranded, respectively. There is a slight increase in the absorbance value at these wavelengths as the irradiation time increases (**Figure 6.15 a)** and **b)**).

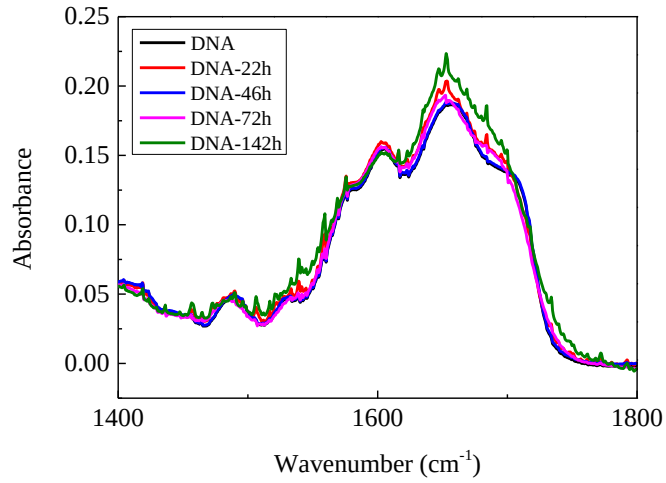

a)

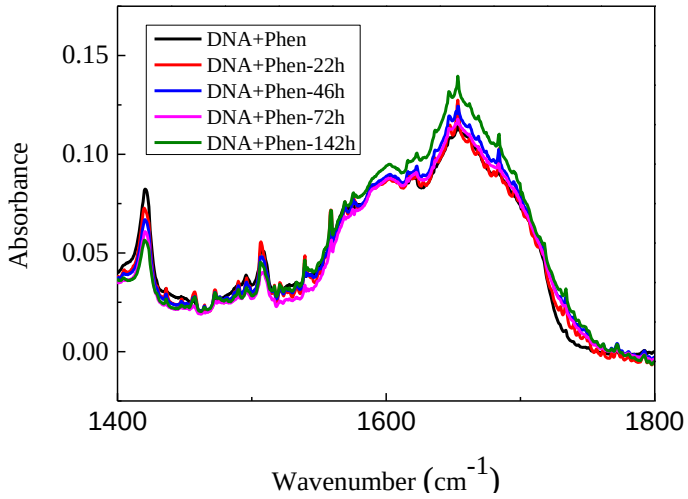

b)

Figure 6.15: Evolution of the absorbance spectra of a) DNA and b) DNA+Phen from 1400 to 1800 cm-1, as the irradiation time increases.

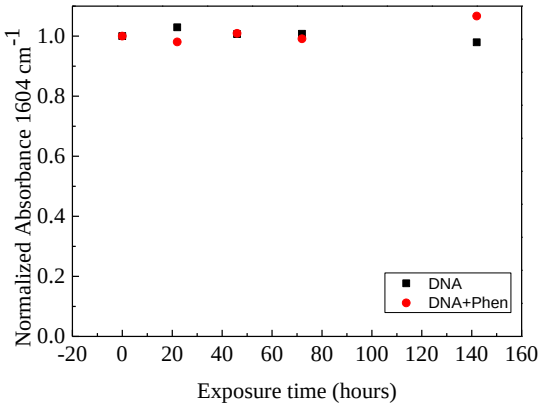

Figure 6.16: Evolution of the peak at 1604 cm^{-1}, of the infrared absorbance spectra of DNA and DNA+Phen cast film as the exposure time to UV radiation increases.

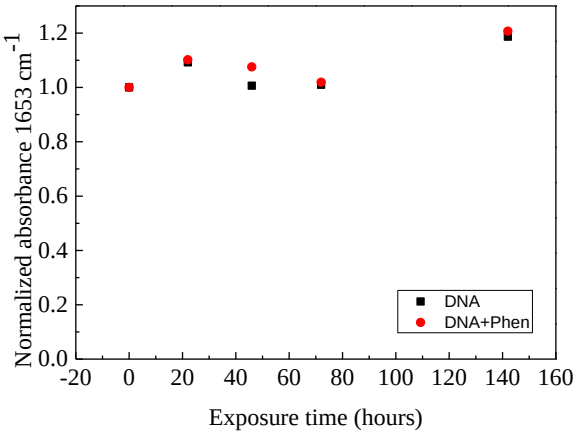

Figure 6.17: Evolution of the peak at 1653 cm^{-1}, of the infrared absorbance spectra of DNA and DNA+Phen cast film as the exposure time to UV radiation increases.

The presence of Phen does not have a significant influence in the evolution of these peaks as shown in **Figure 6.18** and **6.19.** The observed increase in absorbance could be related to the formation of C=C bonds in the case of the peak at 1604 cm^{-1}, and to the formation of C=O bonds for the peak at 1653 cm^{-1} [51].

Table 6.3: Characteristic infrared absorption peaks for DNA and DNA+Phen and the correspondent decaying constant and assignment. The column effect of Phen, indicates the behavior of the peak when the intercalator, 1,10-phenanthroline is present.

Peak (cm^{-1})	**T_{DNA} (hours)**	**$T_{DNA+Phen}$ (hours)**	**Assignment**	**Effect of Phen**
965	135±27	175±43	CC stretch of the backbone	Protection
1015	347±31	270±29	Furanose vibrations	Degradation
1055	574±25	483±68	CO stretch of the furanose backbone	Degradation
1087	306±56	391±90	Symmetric PO_2^- stretching of backbone	Inconclusive (due to the error present)
1232	-	323±40	Antisymmetric PO_2^- stretch in A-form	Inconclusive
1280	104±7	150±24	C5=C6 vibration of cytidine	Protection
1295	96±10	139±30	C4-NH2 strength of cytosine	Protection
1604	-	-	C=N ring vibration of guanine	No effect
1653	-	-	C2=O2 strength of cytosine single stranded or double stranded	No effect

6.3 Conclusions

Cast films prepared with solutions of DNA and DNA+Phen, were irradiated for different periods of time and characterized by infrared spectroscopy in order to analyze the DNA damage caused by UV radiation in the presence of the intercalator Phen.

The DNA damage occurs in the phosphate groups and sugars. Regarding the sugars, there was a decrease in the absorbance as the irradiation time increased, indicating a degradation pattern which was less accentuated in the presence of the intercalator, indicating that Phen has a protective effect on this particular DNA component. Considering the peak assigned to the anti-symmetric PO_2^- stretch in A form, the degradation is much accentuated in the presence of Phen. There was no significant alteration relatively to the furanose, however the presence of Phen lead to a decrease in the absorbance, indicative of degradation. The same was observed for the peak assigned to the CO stretch bond of the furanose backbone, where the presence of Phen increased the degradation.

The peaks assigned to the C5=C6 vibration of cytidine, and to the C4-NH2 strength of cytosine, all showed a decrease in absorbance as the irradiation time increased. The degree of degradation of these functional groups was decreased in the presence of the intercalator, which indicates that Phen may act as a protective agent.

The intercalator showed no effect on the degradation of the peaks assigned to the C=N ring vibration of guanine (1604 cm^{-1}), and to the C2=O2 strength of cytosine single stranded or double stranded (1653 cm^{-1}). The observed increase in absorbance for these peaks is related to the formation of new chemical bonds, namely C=C (for the peak at 1604 cm^{-1}), and C=O (for the peak at 1653 cm^{-1}).

7

Conclusion

7.1 Conclusion

This dissertation had as main objective the study the effect of UV radiation on DNA in the presence of the intercalator 1,10-phenanthroline. This study is of much importance in order to increase the destruction of cancerous cells when irradiated in the presence of the intercalator. The DNA damage was analyzed by VUV, UV-Vis, and FTIR spectroscopy.

The characterization done by VUV of cast films of Phen, and DNA+Phen, demonstrated that the presence of UV had no significant influence on the degradation pattern of the molecules. This indicates that the presence of water is essential in order to observe the effect of UV radiation. The electronic transitions were assigned for each band present in the obtained Phen spectrum.

Aqueous solutions of DNA, Phen, and DNA+Phen were characterized by UV-Vis. The evolution of the absorbance at 260 nm, showed that, even though both DNA and Phen molecules were degraded by UV radiation, the presence of the intercalator had no effect in the degradation of DNA.

The analysis done by FTIR of cast films of DNA, and DNA+Phen, made it possible to identify that DNA damage occurs at the sugars and phosphate groups when exposed to UV radiation. The presence of the intercalator Phen had a protective effect on some DNA components, such as cytosines, and a degradation effect on other DNA components such as the furanose.

It can be concluded that the intercalating agent, 1,10-phenanthroline , is not a good candidate on its own to induce DNA lesions. However, it can form metallic complexes that may cause DNA damage.

7.2 Future Works

In future studies, the effect of UV radiation can be analysed under different atmospheric conditions, for example, by varying that temperature, moisture and oxygen concentration. It would also be pertinent to study the pH variation over time. The obtained cast films could be further analyzed by other techniques, such as, Raman and fluorescence spectroscopy.

References

[1] "Cancer Statistics - National Cancer Institute." [Online]. Available: http://www.cancer.gov/about-cancer/what-is-cancer/statistics. [Accessed: 10-Jul-2015].

[2] A. Favier, M. Blackledge, J. Simorre, S. Crouzy, V. Dabouis, A. Gueiffier, D. Marion, and J. Debouzy, "Solution Structure of 2- (Pyrido [1 , 2- e] purin-4-yl) amino-ethanol Intercalated in the DNA Duplex d (CGATCG) 2 †," pp. 8717–8726, 2001.

[3] B. Neto and A. Lapis, "Recent developments in the chemistry of deoxyribonucleic acid (DNA) intercalators: principles, design, synthesis, applications and trends," *Molecules*, vol. 14, pp. 1725–1746, 2009.

[4] L. Lerman, "Structural Considerations in the Interaction of DNA and Acridines," *J. Mol. Biol.*, vol. 3, no. 1, p. 18, 1961.

[5] N. Wheate, C. Brodie, S. Kemp, and J. Aldrich-Wright, "DNA intercalators in cancer therapy: Organic and inorganic drugs and their spectroscopic tools of analysis," *MINI-REVIEWS Med. Chem.*, vol. 7, pp. 627–648, 2007.

[6] M. Wan and J. Lin, "Current evidence and applications of photodynamic therapy in dermatology," *Dove Med. Press*, vol. 7, pp. 145–163, 2014.

[7] C. Rocha, "Lesões inteligentes em DNA," 2011.

[8] A. Teresa and S. Neves, "Estudo da ação danificadora do 2 , 2 ' -Bipyridyl no DNA presença de radiação UV," 2014.

[9] P. Alberts, B., Bray, D., Hopkin, K., Johnson, A., Lewis, J., Raff, M., Roberts, K., Walker, *Essencial Cell Biology*. Garland Science, 2004.

[10] J. C. García-Ramos, R. Galindo-Murillo, F. Cortés-Guzmán, L. Ruiz-Azuara, C. Conjunto, D. Investigación, and Q. Sustentable, "Metal-Based Drug-DNA Interactions," vol. 57, no. 3, pp. 245–259, 2013.

[11] OpenStax, "DNA Structure and Sequencing." [Online]. Available: http://philschatz.com/biology-book/contents/m44486.html. [Accessed: 03-Jan-2016].

[12] G. P. Pfeifer, Y. You, and A. Besaratinia, "Mutations induced by ultraviolet light.," *Mutat. Res.*, vol. 571, pp. 19–31, 2005.

[13] A. P. Schuch and C. F. M. Menck, "The genotoxic effects of DNA lesions induced by artificial UV-radiation and sunlight.," *J. Photochem. Photobiol. B.*, vol. 99, no. 3, pp. 111–116, 2010.

[14] H. Soehnge, A. Ouhtit, and H. N. Ananthaswamy, “Mechanisms of induction of skin cancer by UV radiation,” *Front. Biosci.*, vol. 2, pp. 538–551, 1997.

[15] “DNA DAMAGE AND REPAIR.” [Online]. Available: http://www.sivabio.50webs.com/dam.htm. [Accessed: 30-Nov-2015].

[16] S. Brown, E. Brown, and I. Walker, “The present and future role of photodynamic therapy in cancer treatment,” *Lancet Oncol.*, vol. 5, pp. 497–508, 2004.

[17] C. a. Robertson, D. H. Evans, and H. Abrahamse, “Photodynamic therapy (PDT): A short review on cellular mechanisms and cancer research applications for PDT,” *J. Photochem. Photobiol. B Biol.*, vol. 96, pp. 1–8, 2009.

[18] A. P. Castano, T. N. Demidova, and M. R. Hamblin, “Mechanisms in photodynamic therapy: part two—cellular signaling, cell metabolism and modes of cell death,” *Photodiagnosis Photodyn. Ther.*, vol. 1, pp. 279–293, 2004.

[19] M. Sirajuddin, S. Ali, and A. Badshah, “Drug-DNA interactions and their study by UV-Visible, fluorescence spectroscopies and cyclic voltametry,” *J. Photochem. Photobiol. B Biol.*, vol. 124, pp. 1–19, 2013.

[20] R. Eckel, R. Ros, A. Ros, S. D. Wilking, N. Sewald, and D. Anselmetti, “Identification of binding mechanisms in single molecule-DNA complexes,” *Biophys. J.*, vol. 85, no. September, pp. 1968–1973, 2003.

[21] E. Sarcoma, “Intercalation (chemistry),” pp. 9–11, 1961.

[22] S. E. Perdiz Daniel, Gróf Pál, Mezzina Mauro, Nikaido Osamu, Moustacchi Ethel, “DISTRIBUTION AND REPAIR OF BIPYRIMIDINE PHOTOPRODUCTS IN SOLAR UV-IRRADIATED MAMMALIAN CELLS. POSSIBLE ROLE OF DEWAR PHOTOPRODUCTS IN SOLAR MUTAGENESIS,” pp. 1–47, 2000.

[23] S. D. C. Rosemary A. Marusak, Kate Doan, *Integrated approach to coordination chemistry : an inorganic laboratory guide*. 2007.

[24] “Product Specification,” p. 63103.

[25] P. L. B. V, “Ultraviolet purification application information,” 2006.

[26] C. Daniel and S. Mota, “DESENVOLVIMENTO DE UM SISTEMA PARA BIOMOLÉCULAS BIOMOLÉCULAS,” 2011.

[27] F. Schmid, “Biological Macromolecules : UV-visable Spectrophotometry,” *Encycl. Life Sci.*, pp. 1–4, 2001.

[28] K. P. C. and N. E. S. Vollhardt, *Organic Chemistry - Structure and Function*, vol. 1. 2002.

[29] C. Solomons, G. Fryhle, *Organic Chemistry*. 2004.

[30] A. Monteiro, “Estudo da dinamica da criação e da relaxação de birrefrigência fotoinduzida em filmes automontados de PAH/PAZO,” FCT-UNL, 2013.

[31] M. K. Denk, “UV-Vis & PES,” 2005. [Online]. Available: http://131.104.156.23/Lectures/CHEM_207/uv-vis.htm. [Accessed: 28-Oct-2015].

[32] C. Würth, M. Grabolle, J. Pauli, M. Spieles, and U. Resch-Genger, “Relative and absolute determination of fluorescence quantum yields of transparent samples.,” *Nat. Protoc.*, vol. 8, no. 8, pp. 1535–50, Aug. 2013.

[33] A. Duarte, P. J. Gomes, J. H. F. Ribeiro, P. Ribeiro, S. V Hoffmann, N. J. Mason, O. N. Oliveira, and M. Raposo, “Characterization of PAH/DPPG layer-by-layer films by VUV spectroscopy.,” *Eur. Phys. J. E. Soft Matter*, vol. 36, p. 98, 2013.

[34] “Specifications of the UV1 beamline.” [Online]. Available: http://www.isa.au.dk/facilities/astrid/beamlines/uv1/uv1OpticalSpecs.asp. [Accessed: 01-Dec-2015].

[35] S. Ege, *Organic Chemistry: Structure and Reactivity*, vol. 2004.

[36] “How an FTIR Spectrometer Operates - Chemwiki.” [Online]. Available: http://chemwiki.ucdavis.edu/Physical_Chemistry/Spectroscopy/Vibrational_Spectroscopy/Infrared_Spectroscopy/How_an_FTIR_Spectrometer_Operates. [Accessed: 10-Jul-2015].

[37] T. Nicolet and C. All, “Introduction to Fourier Transform Infrared Spectrometry,” 2001.

[38] I. Walker, M. Palmer, and A. Hopkirk, “The electronic states of the azines. II. Pyridine, studied by VUV absorption, near-threshold electron energy loss spectroscopy and ab initio multi-reference configuration interaction calculations,” *Chem. Phys.*, vol. 141, no. 2–3, pp. 365–378, 1990.

[39] I. Walker and M. Palmer, “The electronic states of the azines. IV. Pyrazine, studied by VUV absorption, near-threshold electron energy-loss spectroscopy and ab initio multi-reference configuration interaction calculations,” *Chem. Phys.*, vol. 153, no. 1–2, pp. 169–187, 1991.

[40] P. Gomes, “Characterization of Molecular Damage Induced by UV Photons and Carbon Ions on Biomimetic Heterostructures,” FCT-UNL, 2014.

[41] M. Coelho, “Estudo do Efeito da Radiação UV em Filmes de ADN com intercalante,” FCT-UNL, 2008.

[42] R. So and S. Alavi, “Vertical excitation energies for ribose and deoxyribose nucleosides,” *J. Comput. Chem.*, vol. 28, pp. 1776–82, 2007.

[43] M. Shukla and J. Leszczynski, “TDDFT investigation on nucleic acid bases: Comparison with experiments and standard approach,” *J. Comput. Chem.*, vol. 25, pp. 768–78, 2004.

[44] P. J. Gomes, P. a. Ribeiro, D. Shaw, N. J. Mason, and M. Raposo, “UV degradation of deoxyribonucleic acid,” *Polym. Degrad. Stab.*, vol. 94, pp. 2134–2141, 2009.

[45] R. Silverstein, G. Bassler, and T. Morrill, *Spectrometric Identification of Organic Compounds*, 5th ed. 1991.

[46] G. Sharma and A. K. Narula, “Eu(3+), yb (3+) and eu (3+)-yb (3+) complexes with salicylic Acid and 1,10-phenanthroline: synthesis, photoluminescent properties and energy transfer.,” *J. Fluoresc.*, vol. 25, pp. 355–60, 2015.

[47] N. Gault, O. Rigaud, J.-L. Poncy, and J.-L. Lefaix, “Infrared microspectroscopy study of gamma-irradiated and H2O2-treated human cells.,” *Int. J. Radiat. Biol.*, vol. 81, no. 10, pp. 767–79, 2005.

[48] Ö. Tamer, D. Avcı, Y. Atalay, B. Çoşut, Y. Zorlu, M. Erkovan, and Y. Yerli, “Synthesis, X-ray structure, spectroscopic characterization and nonlinear optical properties of triaqua(1,10-phenanthroline-2,9-dicarboxylato)manganese(II) dihydrate: A combined experimental and theoretical study,” *J. Mol. Struct.*, vol. 1100, pp. 605–613, 2015.

[49] Y. Wang, Y. Zhang, D. Zhu, K. Ma, H. Ni, and G. Tang, “Synthesis, structural characterization and theoretical approach of the tri(2-(2,6-dichlorophenyl)-1H-imidazo[4,5-f][1,10]phenanthroline) cobalt(II),” *Spectrochim. Acta Part A Mol. Biomol. Spectrosc.*, vol. 147, pp. 31–42, 2015.

[50] M. Zhao, P. Xi, X. Gu, Z. Li, M. Gao, and B. Cheng, “Synthesis, characterization and fluorescence properties of a novel rare earth complex for anti-counterfeiting material,” *J. Rare Earths*, vol. 28, no. 208005, pp. 75–78, 2010.

[51] B. Stuart, *Infrared Spectroscopy: Fundamentals and Applications*. 2004.